ELECTRONIC STATES AND BAND SPECTRUM STRUCTURE IN DIATOMIC MOLECULES. VII. $^2P \rightarrow {}^2S$ AND $^2S \rightarrow {}^2P$ TRANSITIONS

By Robert S. Mulliken

Abstract

A survey is made of the varied empirical structure-types to be expected for $^2P \rightarrow {}^2S$ and $^2S \rightarrow {}^2P$ bands, and examples of these types are discussed individually. In agreement with Kemble's theory, the arrangement of the rotational levels in the ^2P state changes continuously with the parameter $\Delta E/B$ (ΔE = electronic doublet separation), and these changes are responsible for a large part of the observed variations in band structure. Fig. 1 and Table I show how the arrangement of the ^2P levels changes with $\Delta E/B$, and Figs. 2—5 show, for the MgH, OH, HgH, and NO γ bands, how observed branches are related to energy levels. In Table II, data on ΔE and B are listed for a number of molecules. The mode of variation of the arrangement of the rotational levels in ^2P states appears to be in striking agreement with the quantitative formulas of Hill and Van Vleck. For example, if $\Delta E/B = +2$, their equation becomes formally identical with the Kramers and Pauli formula which holds exactly for the ^2P state of CH.

A *consistent notation*, as proposed in VI of this series, is given here for the known branches of the MgH, CaH, OH, ZnH, CdH, HgH, and NO bands; this notation has already been applied to the OH and BO bands (Kemble, Jenkins) and to CH λ3900. A more or less detailed discussion is given of the spectra mentioned, especially MgH and OH; some term values are given for ^2P and ^2S states of MgH, CaH and OH.

In the bands just mentioned, band-structure and missing lines show good agreement with theory. In the cases where $|\Delta E/B|$ is small for the ^2P state (CH, MgH) there is agreement with the case *b* intensity theory (six main branches, four weak satellite branches). As $|\Delta E/B|$ increases, the satellite branches get stronger, and two new branches become evident. This tendency first appears distinctly in OH, where the satellite branches, although very weak, are much too strong for Hund's case *b*, and where a previously unclassified very weak branch is found to be one of the two new branches just mentioned. As $|\Delta E/B|$ increases still further, the six weak branches finally become equal to the other six in intensity. This metamorphosis has also been discussed by Hulthén. The observed relations, in particular the equality of intensity of the six "weak" and the six "strong" branches when $|\Delta E/B|$ is very large, appear to be in excellent agreement with the quantitative intensity formulas of Hill and Van Vleck.

A conclusion of interest for the empirical study of $^2P \rightarrow {}^2S$ and $^2S \rightarrow {}^2P$ bands is the following: in four-headed bands of these types the *first* head should always be weaker than the rest unless $|\Delta E/B|$ is large, and should disappear if $|\Delta E/B|$ is near zero.

Intensity relations in $^3P \rightarrow {}^3S$, $^3P \rightarrow {}^1S$, and other types of bands are briefly discussed for the case that one electronic state falls under Hund's case *a*, the other under his case *b*; some predictions are made.

Introduction: General Survey of Structure and Intensity Types in $^2P \rightarrow {}^2S$ and $^2S \rightarrow {}^2P$ Bands

THE present and the previous paper (VI)[1] of this series resulted from an attempt to explain in detail a number of spectra which, according to

[1] R. S. Mulliken, Phys. Rev. **30**, 785 (1927); for discussion of magnetic and nuclear kinetic energy relations cf. pp. 793–6.

Hund's theory of molecular electronic states,[2] must be classified as $^2S \rightarrow {}^2P$ and $^2P \rightarrow {}^2S$ transitions,[3] but which exhibit great variety in the obvious features of their structure. These spectra differ especially in regard to (1) the forms of the rotational energy functions which must be assumed to account for the forms of the observed branches, (2) intensity relations, as shown especially by the number of strong branches, which is sometimes six, sometimes twelve, sometimes apparently eight. The explanation of these differences must be sought in variations in the doublet separations and other related characteristics of the ^2S and especially in those of the ^2P states involved.

The object of the following paragraphs is to make a brief qualitative survey of the types which are to be expected theoretically for the structure of bands of the class here considered. This makes it easier to understand the individual examples which are discussed in the later sections of the paper.

Form of rotational terms of ^2P state as a function of $\Delta E/B$. First we consider the possible forms of the rotational energy terms $F_1(j)$ and $F_2(j)$ of the ^2P state. As Kemble has shown, these forms depend essentially on the parameter $\Delta E/B$,[5] where ΔE is the energy-difference between parallel and antiparallel orientations of s with respect to σ_k,[6] and B is the familiar coefficient of the main rotational energy term (both ΔE and B are to be understood below as measured in wave-numbers). For our survey of types we have then to investigate how $F_1(j)$ and $F_2(j)$ behave as a function of $\Delta E/B$. The complication that each level of the F_1 and F_2 sets is really a narrow doublet (σ-type doubling) need not concern us for the present.

If $|\Delta E/B|$ is large, and j not too large, we have Hund's case a. Positive ΔE gives a normal ^2P state, which we shall call ^2P_n, negative ΔE an inverted ^2P, or ^2P_i, state. If $\Delta E \sim 0$, or if j is very large, we have Hund's case b. For intermediate values of $\Delta E/B$ or j there are intermediate cases. The various distinctive cases may be classified according to the notation of Table I, in which the main characteristics of the $F(j)$ functions are given for each such case. The meaning of the notation (e.g., $^2P_{nab}$) should be obvious. The relations given in Table I can all be deduced from the qualitative considerations given in VI (cf. ref. 2, pp. 793–6), together with Kemble's quantitative formulas.[4,7] The same results also follow from the beautiful

[2] F. Hund, Zeits. f. Physik, **36,** 657 (1926); **42,** 93 (1927).

[3] Cf. R. S. Mulliken, Phys. Rev. **29,** 642–3 (1927).

[4] E. C. Kemble, Phys. Rev. **30,** 387 (1927).

[5] $\Delta E/B$ is Kemble's function P. *In general,* $P = A/2Bs^2$, the magnetic energy being $A \cos\theta$, θ being the angle between s and σ_k. Evidently, $\Delta E = 2A$. For $s = \frac{1}{2}$ as in the present case, P reduces to $2A/B$ or $\Delta E/B$.

[6] ΔE is approximately equal in Hund's case a to the observed separation between the lowest F_1 and F_2 levels, but is more difficult to specify in case b, especially in view of the loss of the old literal interpretation of the geometrical relation of σ_k, l, and s in the new quantum mechanics. But cf. Hill and Van Vleck.[7a]

[7] Kemble's results are not in the form of closed formulas applicable to all cases, hence the qualitative considerations of VI are used here, supplemented by the conclusions expressed in Kemble's Eq. (23). But cf. ref. 7*a*.

TABLE I. *Term-form as a function of j for ^2P states, for various values of the parameter $\Delta E/B$. (Footnote numbers here refer to the notes at the bottom of this page.)*

Value of $\Delta E/B$	*Term-form*[1,4]	*Form of ΔF's*[1,3,4]	*F and ΔF relations for moderate j.*[5]	
+large ($^2P_{na}$)	$B[j(j+1)-\sigma_i^2]$, $\sigma_1=\frac{1}{2}$, $\sigma_2=1\frac{1}{2}$ (cf. note 2)	$\Delta_1F(j)=2B(j+1)$ $\Delta_2F(j)=4B(j+\frac{1}{2})$	$F_2(j)-F_1(j+1)=$Const. $>>>0$	$\Delta F_2(j)\backsim\Delta F_1(j)$
>about +10 (+10 is about middle of $^2P_{nab}$ region, which begins at $\Delta E/B=+4$)	$B_i^*[j(j+1)]+\cdots$, with $B_2^*>B>B_1^*$	$\Delta_1F_i(j)=2B_i^*(j+1)+\cdots$ $\Delta_2F_i(j)=4B_i^*(j+\frac{1}{2})+\cdots$	$F_2(j)-F_1(j+1)>>0$, but diminishing with increase of j (cf. note 6)	$\Delta F_1(j+1)>\Delta F_2(j)>\Delta F_1(j)$
+2 (middle of $^2P_{nba}$) region)[7]	$B[\{(j+\frac{1}{2})^2-\sigma_k^2\}^{\frac{1}{2}}\mp\epsilon]^2$, $\sigma_k=1$, $\epsilon=\frac{1}{2}$	Not simple[7]	$F_2(j)-F_1(j+1)<0$; $F_2(j)-F_1(j)>0$ (cf. note 6)	$\Delta F_2(j)>\Delta F_1(j+1)$
$\backsim$0(^2P_b)	$B[j_k(j_k+1)-\sigma_k^2]$, with $j_k=j\pm\frac{1}{2}$	$\Delta_1F(j_k)=2B(j_k+1)$ $\Delta_2F(j_k)=4B(j_k+\frac{1}{2})$	$F_2(j)-F_1(j+1)=0$; $F_2(j)-F_1(j)>0$	$\Delta F_2(j)=\Delta F_1(j+1)$, i.e. $\Delta F_2(j_k)=\Delta F_2(j_k)$
−($^2P_{ia\,b}$)	$B_i^*[j(j+1)]+\cdots$, with $B_2^*>B>B_1^*$	$\Delta_1F_i(j)=2B_i^*(j+1)+\cdots$ $\Delta_2F_i(j)=4B_i^*(j+\frac{1}{2})+\cdots$	$F_2(j)-F_1(j+1)>>0$, but diminishing with increasing j(cf. note 6)	$\Delta F_1(j+1)>\Delta F_2(j)>\Delta F_1(j)$
−large ($^2P_{ia}$)	$B[j(j+1)-\sigma_i^2]$, $\sigma_1=1\frac{1}{2}$, $\sigma_2=\frac{1}{2}$. (cf. note 2)	$\Delta_1F(j)=2B(j+1)$ $\Delta_2F(j)=4B(j+\frac{1}{2})$	$F_2(j)-F_1(j+1)=$Const. $>>>0$	$\Delta F_2(j)\backsim\Delta F_1(j)$

Notes for Table I. (1) The term-form as given is of course incomplete in that small terms in j^4, etc. have been omitted. The j and j_k values in the term-formulas are those of the new mechanics: j = half-integral, j_k = integral, for ^2P.

(2) Although the B^* values should become practically identical for the F_1 and F_2 states as case a is approached (large $|\Delta E/B|$), a small real difference in B values might be expected ultimately to develop if ΔE becomes very large.

(3) By definition (cf. I of this series) $\Delta_2F(j)=F(j+1)-F(j-1)$, while $\Delta_1F(j)=F(j+1)-F(j)$.

(4) It will be noted that Δ_2F should be approximately of the form $C\tau$, with τ = integral or half integral, except in certain regions of small positive values of $\Delta E/B$. When this is the case, the absolute j or j_k numbering, as well as the minimum values of j or j_k, can be determined at once from the empirical Δ_2F's (if τ = integral, we know $\tau=j+\frac{1}{2}$, while if τ = half-integral, $\tau=j_k+\frac{1}{2}$,—cf. note 1 above). This method is still good even when B^* differs considerably from B, but finally fails in the region of small positive $\Delta E/B$ values already mentioned; this region extends a considerable distance[7c] toward case $^2P_{nab}$, from case ^2P_b. Here ΔF_2 is no longer even approximately a linear function of j or j_k (cf. the cases of CH λ3900 in VI, and of MgH, below), and other criteria must be used. In border-line cases (CaH, OH), the relation $\Delta_2F=C\tau$ is only roughly fulfilled, but can be used subject to confirmation by other methods.—Similar relations hold for Δ_1F (cf. note 3).

(5) The relations given in the last column hold for Δ_1F's as well as for Δ_2F's, at least if σ-type doubling is neglected.

(6) In the fourth column, the differences $F_2(j)-F_1(j+1)$ in the intermediate cases $^2P_{nab}$, $^2P_{nba}$, and $^2P_{iab}$, tend toward zero as j increases; cf. ref. 7*b* for exact formula; but this formula is subject to correction for the effects of the magnetic field developed by rotation (cf. Kemble, ref. 4, top p. 395).

(7) For the relations in this case, cf. discussion of CHλ3900 in VI. The Kramers and Pauli term-form here now proves to be exactly the form which Hill and Van Vleck's formula[7b] assumes for $\Delta E/B=+2.00$.

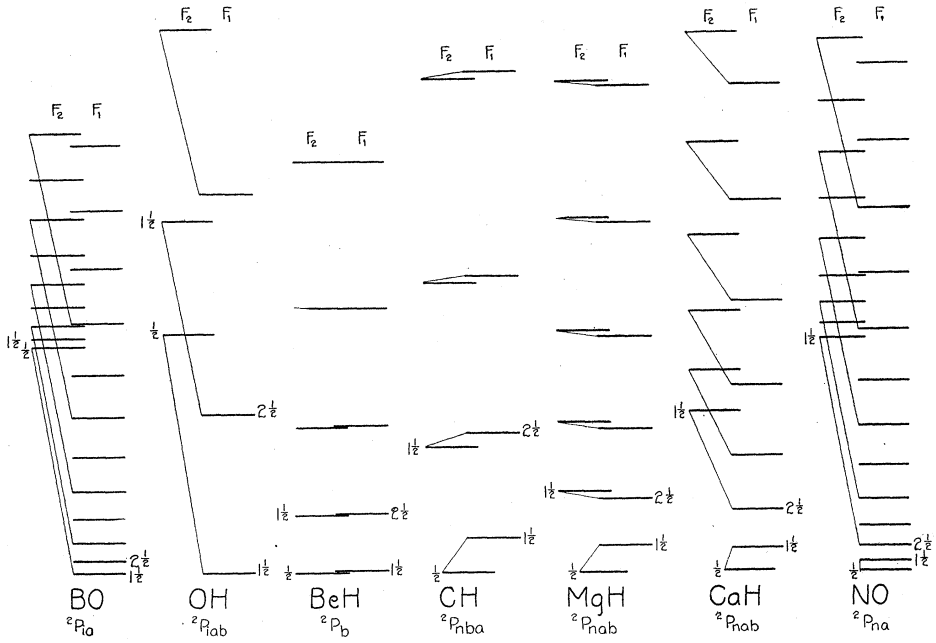

Fig. 1 shows, on a uniform scale, with the lowest level placed at zero in each case, the arrangement and spacing of the rotational levels of a number of ^2P states having a variety of values of ΔE and B (cf. Tables I and II for more complete data and explanation of designations such as $^2P_{iA}$, $^2P_{nba}$). The numbers opposite some of the levels are j values. The spacings of the levels are for the vibrational quantum number $n=0$, except that in the case of NO they are for $n=4$. F_1 and F_2 levels which would in case b correspond to the same value of j_k are indicated by slanting connecting lines. The level $F(\frac{1}{2})$, which is classified as $F_2(\frac{1}{2})$ for negative values of $\Delta E/B$, soon becomes obviously associated with the F_1 levels as $\Delta E/B$ becomes increasingly positive, and is then naturally classified as $F_1(\frac{1}{2})$. The level $F(\frac{1}{2})$ is accordingly represented in Fig. 1 as shifting gradually from the F_2 set to the F_1 set of levels.[7d] The reader may find it of interest to compare and correlate the varying patterns of levels shown in Fig. 1 with the varying relative orientations and interaction energies of the σ_k and s vectors. A discussion of the latter will be found in ref. 1 (cf. Fig. 1 and pp. 793–6) and in ref. 4. The $F_1(j)$ and $F_2(j)$ data used are mainly quantitative data which either are given in this paper (MgH, CaH) or have been obtained in obvious ways with the help of published ΔF data (BO, ref. 11; OH, Dieke, ref. 31; NO, ref. 41). For BeH, the spacings of the levels have merely been estimated roughly by assuming $F(j_k)=7.82[j_k(j_k+1)-\sigma_k^2]$, the value $B=7.82$ having been obtained from Petersen's value of the moment of inertia (Abstract 86, April 1928 meeting of Am. Phys. Soc.); the separations $F_1(j+1)-F_2(j)$ here are very small and not yet accuratey known, and the spacings are exaggerated. In Petersen's BeH bands, (cf. also Watson, Abstract 85), the type of transition is not certain, but probably either the initial, or the final, state is ^2P, and since $B'\sim B''$ in these bands, the above representation should be not far wrong.

[7c] At $\Delta E/B=+4$ (boundary of $^2P_{nba}$ and $^2P_{nab}$ regions), according to Hill and Van Vleck's formula,[7b] the term form is the same as for $\Delta E/B=0$; hence near *both* these points we expect $\Delta_2 F\backsim C\tau$, with $\tau=$half-integral. But inside each of the regions $^2P_{nba}$ and $^2P_{nba}$ (cf. CH, with $\Delta E/B=+2$, and MgH, with $\Delta E/B\backsim 6$), $\Delta_2 F$ is no longer even approximately of the form $C\tau$.

[7d] In Hill and Van Vleck's formula[7b], $F(\frac{1}{2})$ must be classified as $F_2(\frac{1}{2})$ from $\Delta E/B=-\infty$ to $+2$, and as $F_1(\frac{1}{2})$ for $\Delta E/B>+2$.

work of Hill and Van Vleck[7a] who, with the new quantum mechanics, have recently obtained a closed formula giving the energy quantitatively throughout the entire range of $\Delta E/B$ values.[7b].

The changing associations and spacings of the rotational levels as $\Delta E/B$ is varied can best be understood with the help of Fig. 1, in which observed levels are shown for a number of *actual examples* of ^2P states; these examples are individually discussed below, or elsewhere. The gradual shift of the $F(\frac{1}{2})$ level (cf. refs. 2 and 4) from its association with the F_2 levels in $^2P_{ia}$ and ^2P_b states to association with the F_1 levels in $^2P_{na}$ states is especially well shown.

TABLE II. *Examples of ^2P states arranged according to $\Delta E/B$ values.*

Case	Molecule	ΔE	B_1*	B_2*	B	$\Delta E/B$	Bands	Diagram
$^2P_{na}$	HgH	3683	6.56	6.61	6.58	+560	$P\rightarrow S$	Fig. 4
	CdH	1001	5.96	6.03	5.99	+169	$P\rightarrow S$	(Type of Fig. 4)
	NO	124	1.675	1.724	1.70	+73	$S\rightarrow P$	Figs. 1, 5.
	ZnH	330	7.15	7.47	7.3	+45	$P\rightarrow S$	(Type of Fig. 4)
	NO	33	1.070	1.168	1.12	+29	$P\rightarrow P$	(Data, ref. 9)
	CaH	80	4.09	4.49	4.3	+19	$P\rightarrow S$	Fig. 1
$^2P_{nab}$	MgH	35	—	—	6.1	+5.7	$P\rightarrow S$	Figs. 1, 2.
$^2P_{nba}$	CH	28.4	14.19		14.19	+2.00	$S\rightarrow P$	Fig. 1; and Ref 2, Fig. 3.
$^2P_{iab}$	OH	−127	16.60	20.56	18.47	−6.9	$S\rightarrow P$	Figs. 1, 3.
	CN	−54	—		(1.6)	(−34)	$P\rightarrow S$	
	CO^+	−126	—		(1.6)	(−79)	$P\rightarrow S$	(BO type)
$^2P_{ia}$	$B^{11}O$	−126	1.383	1.412	1.40	−90	$P\rightarrow S$	Fig. 1 and ref. 11

Notes for Table II. (1) The data on ΔE and B^* can be found mainly in the following references: ZnH, CdH, HgH, ref. 8; NO (data from β bands), ref. 9; CaH, ref. 10; MgH, see following detailed treatment for references; CH, ref. 2; OH, see below; CN, CO^+, ref. 10a; $B^{11}O$, ref. 11. The ΔE values used (except for CH and MgH) are merely the empirical values of the interval between the lowest F_1 and the lowest F_2 level, and are perhaps not the most appropriate[6]; the ΔE values given for MgH and CH are so chosen as to make the experimental F data fit Hill and Van Vleck's formula[7b] (cf. Table I, note 7).

(2) The B values given are mostly averages of the B_1* and B_2* values; they should then be moderately accurate, according to Kemble's work[4] on OH.

(3) Under "Bands" is recorded the type of transition ($^2S\rightarrow{}^2P$ or $^2P\rightarrow{}^2S$) in which the given ^2P state has been observed.

(4) Under "Diagram" a reference is given to a figure showing the observed energy levels and transitions (cf. discussion of "Line and level types," below); unless otherwise stated, the figure is to be found in the present paper.

[7a] E. L. Hill and J. H. Van Vleck, Phys. Rev., **32,** 250, 1928. The writer is greatly indebted to Prof. Van Vleck for the opportunity to examine this work before publication. Unfortunately this was not possible before receipt of the proof of the present paper, so that use of Hill and Van Vleck's results could be made only incompletely, in minor changes and additions in the proof.

[7b] Cf. Eq. (27) of Hill and Van Vleck. λ of Hill and Van Vleck is the same as $\Delta E/B$ here. The j_1 and j_2 rotational states of Hill and Van Vleck are respectively identical with the F_2 and F_1 states of the present and previous papers of this series.

[8] R. S. Mulliken, Proc. Nat. Acad. Sci., **12,** 151 (1926).

[9] F. A. Jenkins, H. A. Barton, and R. S. Mulliken, Phys. Rev. **30,** 150 (1927).

[10] E. Hulthén, Phys. Rev. **29,** 97 (1927).

[10a] For data on CO^+ and CN, cf. R. S. Mulliken, Phys. Rev. **26,** 571 (1925). The value of B for CN is estimated by means of the rule that ω_0/B is roughly a constant for the various electronic states of one molecule (R. Mecke, Zeits. f. Physik, **32,** 823, 1925).

[11] F. A. Jenkins, Proc. Nat. Acad. Sci. **13,** 496 (1927). The separation of the F_1 and F_2 sets of levels in Jenkins' Fig. 1 is not to scale.

The changing order of corresponding F_1 and F_2 levels in passing through the $^2P_{nba}$ neighborhood, from $F_2(j) > F_1(j+1)$ to $F_1(j+1) > F_2(j)$ and back, is also clearly shown.

Further information concerning the ^2P states of Fig. 1, and others, is given in Table II. The divergence of B_1^* from B_2^* (cf. ref. 4 and Table I for the meaning of these coefficients), in agreement with Kemble's theory, for intermediate values of $\Delta E/B$, is well shown by the data in Table II. The fact that, in agreement with Kemble's theory, $\Delta E/B$ and not ΔE is the parameter which determines the behavior of a ^2P state for a given range of j values, will be evident if one compares OH and BO (or CaH and NO) in Fig. 1 and in Table II. For the physical reason behind this fact, reference may be made to Kemble's paper. The same fact is also shown in the existence of a continuous variation of intensity relations, in $^2P \rightarrow {}^2S$ and $^2S \rightarrow {}^2P$ bands, as the parameter $\Delta E/B$ changes. These intensity relations are discussed in the following paragraphs.

Intensity relations and number of branches as a function of $\Delta E/B$ of ^2P state. The intensity relations in $^2P \rightarrow {}^2S$ and $^2S \rightarrow {}^2P$ transitions can be predicted by means of the theoretical equations given in VI, if $|\Delta E/B|$ is small for the ^2P state, so that both initial and final state fall to a good approximation under Hund's case *b*. The theory then predicts six strong branches accompanied by four satellite branches of very low intensity.

When $|\Delta E/B|$ is large for the ^2P state, the latter falls under Hund's case *a*, while the ^2S state, as always,[12] falls under case *b*. For such a mixed (*a*,*b*) transition, neither the intensity theory for case *a* transitions (cf. III of this series[13]) nor that for case *b* transitions as given in VI, is applicable. Empirically, however, it is found that as $|\Delta E/B|$ increases there is a gradual transition from the case *b* type with six strong branches (example CH λ3900, with $\Delta E/B = 2.0$) to a type with twelve strong branches (HgH bands, with $\Delta E/B = 560$). In the MgH, OH, and CaH bands ($\Delta E/B \sim +5.7$, -6.9, and $+19$ respectively), the intensity relations of case *b* are still essentially true, there being only six strong branches. But in the OH bands—presumably also in the MgH and CaH bands, but these are less well known—the four satellite branches, whose intensity in case *b* should fall to negligible values as j_k increases, have an appreciable, although still very small, intensity even for large values of j. Also, in OH, at least one new branch makes its appearance, in low intensity. In the ZnH bands ($\Delta E/B \sim +45$) the four satellite branches are perhaps nearly half as strong as the six main branches,[14] and are accompanied by two about equally strong new branches; these (one of which corresponds to the new branch in OH) are branches which in case *b* should be completely absent because they would involve $\Delta j_k = \pm 2$. In the NO γ, BO α, and CdH bands ($\Delta E/B \sim +73$, -90, and $+169$, respectively), the six weaker branches make further gains, and in HgH ($\Delta E/B = +560$) they are approximately equal in intensity to the other six branches. It is

[12] Cf. R. S. Mulliken, Phys. Rev. **30**, 138 (1927).
[13] R. S. Mulliken, Phys. Rev. **29**, 391 (1927).
[14] E. Hulthén, Zeits. f. Physik **45**, 335 (1927).

evident that in the limit of very large $|\Delta E/B|$ the intensities depend on Δj and not at all on Δj_k, j_k having now completely lost its rôle as a quantum number. The twelve observed strong branches represent merely all the possible combinations between ^2P and ^2S levels which satisfy the rule $\Delta j = 0, \pm 1$.

The above relations have been sketched in two preliminary abstracts,[15] and also in a paper by Hulthén.[14] Hulthén has given a partial explanation of them in terms of the correspondence principle. Van Vleck and Hill[7a] have now given theoretical intensity formulas good for the whole range of values of $\Delta E/B$. These have not yet been tested for intermediate values of $|\Delta E/B|$, but agree with the observed relations for very large $|\Delta E/B|$ as in HgH, hence presumably also for the intermediate values.

Throughout the entire range of $\Delta E/B$ values for the ^2P state, σ-type doubling exists for the latter, but on account of certain typical selection rules which evidently remain valid throughout, is prevented from increasing the number of branches. Without these selection rules, one would expect twelve strong branches for small $\Delta E/B$, twenty-four for large $\Delta E/B$. In the OH bands, to be sure (cf. detailed discussion below), certain additional branches are found which run counter to these rules, but they are very weak.

Apparent eight-branch bands of $^2S \rightarrow {}^2P$ and $^2P \rightarrow {}^2S$ types. In certain cases where $|\Delta E/B|$ is large there appear to be only eight instead of twelve branches (BO α bands, CO^+ comet-tail, red CN, NO γ bands). This condition has been shown previously[17] to result from an almost exact coincidence of F_1 and F_2 levels of the ^2S state. The reason this reduces the apparent number of branches from twelve to eight will be clear from a study of diagrams such as Figs. 2–4 below and Fig. 1 of Jenkins' paper on the BO α bands.[11] Essentially, the four satellite branches ${}^QR_{12}$, ${}^PQ_{12}$, ${}^RQ_{21}$, and ${}^QP_{21}$ coalesce each with its corresponding main branch.

The two branches (${}^{PP}P_{12}$ and ${}^{RR}R_{21}$) which correspond to $\Delta j_k = \pm 2$ never coalesce with other branches. Thus when there is coalescence of main and satellite branches the total number of visible independent branches is eight if $|\Delta E/B|$ is large enough to bring out the P_{12} and R_{21} branches (examples, BO α and NO γ bands); otherwise it is six (examples, CH, MgH bands).—As Hulthén has shown,[14] approximate coincidence of F_1 and F_2 levels of the ^2S state occurs in molecules for which ΔE (not $\Delta E/B$) is small in the ^2P state.

Survey of line and level types in $^2P \rightarrow {}^2S$ and $^2S \rightarrow {}^2P$ bands. The possible empirical types of $^2P \rightarrow {}^2S$ and $^2S \rightarrow {}^2P$ bands may be classified according to (*a*) whether the ^2P state is initial or final, (*b*) the sign and magnitude of $\Delta E/B$ of the ^2P state, (*c*) whether or not the F_1 and F_2 levels of the ^2S state are practically coincident. The structure of such bands, and the com-

[15] R. S. Mulliken, Phys. Rev. **29,** 921*A* (1927); **31,** 310*A* (1928).

[16] Cf. II, IV, and especially VI of this series, and theoretical papers of Hund (Zeits. f. Physik **42,** 111, 1927) and of R. de L. Kronig (Zeits. f. Physik **46,** 814, 1928).

[17] R. S. Mulliken, Phys. Rev. **28,** 1218–20 (1926); cf. also F. Hund, Zeits. f. Physik **42,** 99 (1927), and E. Hulthén, ref. 10.

bination relations, combination defects, missing lines, and so on, are much more readily understood with the help of diagrams of rotational energy levels and transitions than in any other way. Hence it seems desirable that such diagrams should be on record for the band-types likely to be found most frequently in practise. Diagrams for a number of representative examples are therefore given in the figures of the present paper, and others are available elsewhere (cf. references in Table II under "Diagram").

The following points may be helpful to the reader in studying these examples: (1) *In all cases* the possible branches are limited to the following: P_1, Q_1, R_1, P_2, Q_2, R_2 (strong branches always); ${}^{Q}R_{12}$, ${}^{P}Q_{12}$, ${}^{R}Q_{21}$, ${}^{Q}P_{21}$ (satellite branches, very weak if $\Delta E/B$ is small, strong if it is large); ${}^{PP}P_{12}$, ${}^{RR}R_{21}$ (absent if $\Delta E=0$, strong if $\Delta E/B$ is large). The notation is that of VI, extended in the case of the last two branches to indicate, by RR or PP, that these branches would correspond in case b to $\Delta j_k=\pm 2$. (2) In ${}^2P\rightarrow{}^2S$ transitions the allocation of given-named satellite branches to main branches is different than in ${}^2S\rightarrow{}^2P$ transitions, e.g., ${}^{P}Q_{12}$ is satellite to P_1 in ${}^2P\rightarrow{}^2S$, but to P_2 in ${}^2S\rightarrow{}^2P$ transitions. (3) The value of j for the first line in any given-named branch differs in many cases for ${}^2P\rightarrow{}^2S$ and ${}^2S\rightarrow{}^2P$, often also (because of the shift of $F(\frac{1}{2})$ from the F_1 to the F_2 series of levels) for an inverted as compared with a normal ${}^2P$ state. (4) For an inverted case a ${}^2P$ state like that in BO the F_1 levels and F_2 levels respectively correspond to ${}^2P_{1\ 1/2}$ and ${}^2P_{1/2}$ electron states, whereas for a *normal* case a ${}^2P$ state as in NO or HgH, they correspond to ${}^2P_{1/2}$ and ${}^2P_{1\ 1/2}$ electron states respectively.

Prediction of Intensity Relations for ${}^3P\rightarrow{}^3S$ and Other Transitions

The present section is a digression from the discussion of ${}^2P\rightarrow{}^2S$ and ${}^2S\rightarrow{}^2P$ transitions. It is, however, an outgrowth of the material of the previous section, and rounds out the discussion of intensity relations given in the papers of this series.

In ${}^3P\rightarrow{}^3S$ bands, nine strong main branches and a number of weak satellite branches are expected if the ${}^3P$ state falls under Hund's case b. The theoretical intensities could be calculated, if desired, by the methods used in V and VI.[17a] The NH bands as analyzed by Hulthén and Nakamura[18] are an example of this type. Here $|\Delta E|$ is roughly 60, B$\sim$15, hence $|\Delta E/4B|$, which for triplet states[5] takes the place of $\Delta E/B$ for doublet states, has approximately the value 1. With increasing values of $(\Delta E/4B)$ in the ${}^3P$ state in ${}^3P\rightarrow{}^3S$ and ${}^3S\rightarrow{}^3P$ transitions, we may, by analogy with ${}^2P\rightarrow{}^2S$ and ${}^2S\rightarrow{}^2P$ bands, expect to find increasing intensity of satellite branches. For large $|\Delta E/4B|$ we may then perhaps expect the appearance in high intensity of all the branches, 24 in number, which conform to the rule $\Delta j=0,\ \pm 1$ and to the selection rules of σ-type doubling.[17a]

Similar considerations doubtless apply to other bands, such as ${}^4P\rightarrow{}^4S$, involving combinations of P and S states. Presumably they apply,[17a] even in cases not involving S states, whenever one state falls under Hund's case a,

[17a] Cf. also ref. 7*a*.

[18] E. Hulthén and S. Nakamura, Nature, Feb. 12, 1927.

the other under Hund's case b. We have in general three limiting cases to consider: (1) Both states fall under case a; (2) one state falls under case a, the other under case b; (3) both states fall under case b. The predicted strong branches are the same for case (1) as for case (3), but in case (1) satellite branches should be strictly absent, while in case (3) such branches should be present in low intensity.[19] In well-developed case (2) the satellite and certain other branches presumably become intense. The NO β bands ($^2P \rightarrow {}^2P$) agree in their intensity relations[20] with case (1), although the $\Delta E/B$ values ($+29$ for the initial, $+73$ for the final state) suggest that a tendency toward case (2) might have been observed.

For an intersystem combination such as $^3P \rightarrow {}^1S$, it is not clear what is to be expected. The fact that ^1S may be classified under either case a or case b makes it difficult to decide how it should behave here. At any rate, the maximum possible number of branches satisfying $\Delta j = 0, \pm 1$ is nine, in three groups, $^3P_2 \rightarrow {}^1S$, $^3P_1 \rightarrow {}^1S$, $^3P_0 \rightarrow {}^1S$. The objection might be raised that σ changes by 2 in $^3P_2 \rightarrow {}^1S$, but this objection probably is not valid, since σ is merely the sum of σ_k and σ_s and is not important as a quantum number. Empirically it appears, from what is known of the band structure, that all the levels $^3P_2$, $^3P_1$, and $^3P_0$ combine with ^1S in the Cameron CO bands.[21,22]

The MgH Bands

Structure and interpretation: general. The green MgH bands, first measured by Fowler[23] and later classed by Heurlinger[24] with the OH bands as typical doublet bands, have more recently been remeasured and analyzed by Watson and Rudnick.[25,26] That the bands are actually due to MgH is satisfactorily shown, in confirmation of other evidence, by the isotope effect.[25,26]

[19] In case (1) the Hönl and London intensity formulas (cf. ref. 13) are applicable, supplemented by Hund's selection rule $\Delta\sigma_s = 0$ (cf. Hund, ref. 1, 1926, and IV of this series: Phys. Rev. **29,** 637, 1927). In case (3), Eqs. (8)–(13) of VI apply.

[20] F. A. Jenkins, H. A. Barton, and R. S. Mulliken, Phys. Rev. **30,** 175 (1927).

[21] Cf. R. T. Birge, Phys. Rev. **28,** 1157 (1926).

[22] But in the red Na_2 bands, which are also thought to be $^3P \rightarrow {}^1S$, each band appears to have only one head, suggesting a limitation to $^3P_1 \rightarrow {}^1S$ (cf. R. Ritschl and D. Villars, Naturwiss., **16,** 219, 1928). No reason is evident for such a contrast between the CO and the Na_2 bands, since $\Delta E/B$ is probably of the same order of magnitude in both.

It is possible that this anomaly can be avoided as follows. The green Na_2 bands ($^1P \rightarrow {}^1S$) and the red bands have a common final ^1S state which on dissociation gives two unexcited (^2S) Na atoms. The initial state of both green and red bands gives on dissociation a ^2P and a ^2S atom (F. W. Loomis, Phys. Rev. **31,** 323, 1928). Now there are four molecular states which are theoretically derivable from a ^2P and a ^2S atom, namely ^3P, ^3S, ^1P, and ^1S. Thus it is possible that the initial state of the red bands may be ^1S (or ^3S) rather than ^3P, so that the bands are $S \rightarrow {}^1S$. Certain features of the bands seem to be in disagreement with this suggestion, however, according to a private communication from Professor Loomis. The question can probably be settled only by a detailed analysis.

[23] A. Fowler, Phil. Trans. Roy. Soc., **209A,** 447 (1909).

[24] T. Heurlinger, Dissertation Lund, 1918.

[25] W. W. Watson and P. Rudnick, Astrophys. J. **63,** 20 (1926).

[26] W. W. Watson and P. Rudnick, Phys. Rev. **29,** 413 (1927).

Each band has three pairs of branches P_1, P_2; Q_1, Q_2; R_1, R_2. Pairs of lines such as $P_1(m)$ and $P_2(m)$, in the notation used by previous workers, form rather narrow doublets which slowly become narrower as m increases. These characteristics are exactly those expected for a case b $^2S \rightarrow {}^2P$ or $^2P \rightarrow {}^2S$ transition. The missing lines and the forms of the $\Delta_2 F''$s and $\Delta_2 F'''$s give evidence (see below) that the transition is $^2P \rightarrow {}^2S$; data on the relative intensities of the P, Q, and R branches, which would give further support to this classification, are not recorded by Watson and Rudnick.

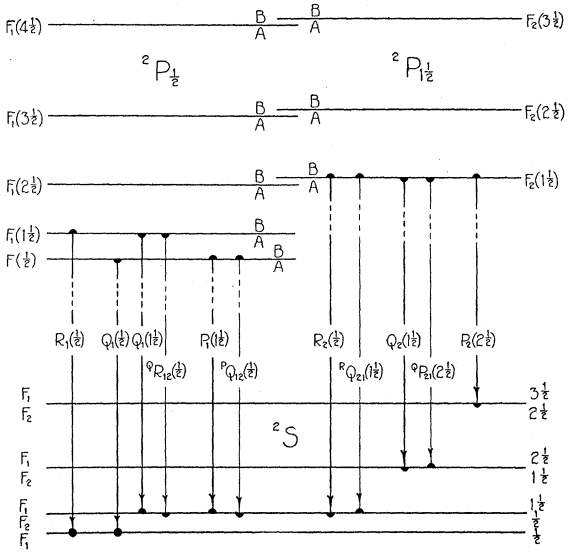

Fig. 2. *Lowest rotational levels, and first line of each branch, for MgH* λ5211 (0, 0 *band*). The levels are drawn to scale from the F' data of Table III (but cf. note *a* of Table III in regard to the level $F_2(1\frac{1}{2})$), and (cf. text, p. 399) from the equation $F''(j_k) = 5.710\, j_k(j_k+1)$. The σ-type doubling is negligibly small on the scale employed, and is shown only by the use of double designations for the levels. Similar remarks apply to the ρ-type doubling in the ^2S levels. On account of the absence (within experimental error) of doubling in the ^2S levels, each satellite branch (light vertical lines in Fig. 2) coincides with one of the main branches (strong vertical lines). The way in which the doublets observed in the spectrum are related to the rotational levels can be seen by drawing additional lines in Fig. 1; e.g. $R_1(1\frac{1}{2})$ forms a doublet with $R_2(\frac{1}{2})$, $Q_1(2\frac{1}{2})$ with $Q_1(1\frac{1}{2})$; $P_1(3\frac{1}{2})$ with $P_2(2\frac{1}{2})$. It may be noted that if the ^2P level $F(\frac{1}{2})$ were here classified as $F_2(\frac{1}{2})$ rather than as $F_1(\frac{1}{2})$, the designations of the lines $Q_1(\frac{1}{2})$, $P_1(1\frac{1}{2})$, and $^PQ_{12}(\frac{1}{2})$ would be altered, to $^RQ_{21}(\frac{1}{2})$, $^QP_{21}(1\frac{1}{2})$, and $Q_2(\frac{1}{2})$. The designations for the ^2P levels of the CH molecule, in VI, were made on the basis of the classification of $F(\frac{1}{2})$ as $F_2(\frac{1}{2})$.[7d]

The observed six branches can be quantitatively explained by the system of energy levels shown in Fig. 2, together with the usual selection rules (cf. VI). The observed branches are evidently the "main" branches, four of them presumably with superposed weak satellite series (these should be unresolved, since $F_1''(j+1) \sim F_2''(j)$ for the ^2S state (see below)). Watson and Rudnick report, without giving data, that there are also independent weak satellite series; these may perhaps correspond to the irregular satellites

in OH which run counter to the selection rules of σ-type doubling. By good luck, the designations P_1, Q_1, R_1, P_2, Q_2, and R_2 used by previous workers can be adopted here without change. The m numbering previously used is, however, to be replaced, by means of the following relations: in the P_1, Q_1, and R_1 branches, $m=j_k''+1=j''+\frac{1}{2}$; in the P_2, Q_2, and R_2 branches, $m=j_k''+1=j''+1\frac{1}{2}$. The j' and j_k' numberings follow, since we know Δj and Δj_k ($\Delta j=\Delta j_k$ here) for each branch.

The relations shown in Fig. 2 are essentially the same as those in CH λ3900 (cf. Fig. 3 of VI[1]), except that (*a*), the change from a $^2S\rightarrow{}^2P$ to a $^2P\rightarrow{}^2S$ transition produces characteristic changes in respect to the first lines of the various branches, and (*b*), in MgH, evidently because of the greater value of $\Delta E/B$, the ^2P $F(\frac{1}{2})$ level is now obviously associated with the F_1 set of levels and so is naturally classed as $F_1(\frac{1}{2})$ rather than as $F_2(\frac{1}{2})$, whereas in CH the classification as $F_2(\frac{1}{2})$ seems the more natural.[7d]

Intensity anomaly in P_2, Q_2, and R_2 branches. According to the intensity theory for case *b*,[1] the lines of the P_2, Q_2 and R_2 branches should be somewhat weaker—approximately in the ratio of the mean j values—than corresponding lines[27] of the P_1, Q_1, and R_1 branches. This of course gives asymptotic equality of intensity of doublet components for high j values. The observed relations are in agreement with these predictions, except that the intensity inequality for low j values is more pronounced than expected; in fact, the first line of each of the branches P_2, Q_2, and R_2 (involving in each case $F_2'(1\frac{1}{2})$) is so weak as to have escaped observation.[25] The CaH bands (see below), with a larger $\Delta E/B$, show a similar but less marked weakness of the early F_2 lines, none of them being too weak to observe except in the Q_2 branch; in molecules with larger values of $\Delta E/B$ the anomaly is no longer noticeable. The explanation of these anomalies is not evident, but they are presumably characteristic of the transition from a case *b* to a case *a* ^2P state.

Empirical justification of interpretation given. While the system of energy levels shown in Fig. 2, plus the selection rules there assumed, is *sufficient* to account for the observed band structure and is in agreement with the theory, it is desirable to show so far as possible that the interpretation given is empirically, with a minimum of theory, a *necessary* one. This requires the investigation of various combination relations.

Empirically, "internal" combination relations such as

$$[RQ_i''\equiv R_i(j)-Q_i(j+1)]=[QP_i''\equiv Q_i(j)-P_i(j+1)]=\Delta_1F_i''(j) \tag{1}$$

and

$$[RQ_i'\equiv R_i(j)-Q_i(j)]=[QP_i'\equiv Q_i(j+1)-P_i(j+1)]=\Delta_1F_i'(j) \tag{2}$$

with $i=1$ or 2, are very nearly, but not quite, fulfilled (cf. ref. 25, Table I, and ref. 26); RQ_i'' etc. here are merely abbreviations for $R-Q$, etc. In explanation of these slight combination defects, Watson and Rudnick assumed, in analogy to Dieke's interpretation of the OH bands, the existence of a fine-scale doubling in all the initial, ^2P, levels (cf. Fig. 2), such that P_i, Q_i, and R_i branches have common final levels, but that the Q_i branches come from slightly displaced levels (F_{iA}' levels) as compared with the P_i and R_i branches (F_{iB}' levels).

In order to justify this scheme empirically, it is necessary to show, (*a*), that P_i, Q_i, and R_i branches actually have common final levels; (*b*), that P_i and R_i branches have common initial levels. This can be done only by means of "external" combination relations, i.e., the demonstration of suitable equalities between sets of combination differences obtained from three

[27] Corresponding lines have equal j_k values and form the obvious doublets of ref. 25.

different bands such as (n_a', n_a''), (n_a', n_b''), (n_b', n_a''). Watson and Rudnick have measured and analyzed the (0, 0), (1, 0), (1, 1), and (0, 1) bands, but unfortunately give wave number data only on the λ5211 (0, 0) band. These are supplemented by a few sets of combination differences from the other bands. The equality,—within experimental error, but not altogether satisfactory (cf. Table II of ref. 26),—of combination differences $Q_1(j)-P_1(j)$ in the (0, 0) and (0, 1) bands furnishes (cf. Fig. 2) the desired verification of the assumption that $P_1(j)$ and $Q_1(j)$ have a common final state. No published evidence is available to show that $R_1(j)$ has also the same final state, nor that $P_2(j)$, $Q_2(j)$, and $R_2(j)$ have a common final state, nor that $P_i(j+2)$ and $R_i(j)$ have a common initial state. Watson and Rudnick indicate, however, that they have tested such relations, and in ref. 26 they give sets of Δ_2F' and Δ_2F'' values for λ5211 which presuppose the validity of such relations.

The fact that the P_1, Q_1, and R_1 branches belong together, and share neither initial nor final states with the likewise coherent P_2, Q_2, and R_2 branches, is only very incompletely established by the published data.

Assignments for j and j_k cannot be made here on the basis of the term forms alone, since the ΔF values of the initial state are not of a simple type (cf. F' data of Table III). The form of the ΔF's of the final state shows, however—cf. below— that this is the ^2S state. If then we agree that the observed lines are "main branch" lines, the restrictions $j' \not< \frac{1}{2}$, $j'' \not< \frac{1}{2}$, $\Delta j = 0, \pm 1$ are sufficient to determine the j and j_k values for the P_1, Q_1, and R_1 branches, and to show that the subscript 1 is rightly used here. The assignments for the P_2, Q_2, and R_2 branches readily follow, if the obvious doublets are interpreted as is required for a $^2P \rightarrow {}^2S$ transition in which the ^2P states closely approach case b for high j values.

Rotational terms of final (^2S) states. Assuming, in spite of the incomplete empirical justification, that the interpretation given in Fig. 2 is correct, we can investigate some of the quantitative relations of F_1 and F_2 terms. Watson and Rudnick's Δ_2F'' values for λ5211[26] are of the form $F_i''(j_k+1) - F_i''(j_k-1) \sim 4B(j_k+\frac{1}{2})$, with $B \sim 5.71$ and $j_k = 1, 2, 3, \cdots$ (except that $j_k = 1$ and 2 are missing for F_2). This corresponds to $F_i''(j_k) = Bj_k(j_k+1) + \cdots$, with $j_k = 0, 1, 2, \cdots$, as expected for a ^2S state. The F_1'' values are probably slightly greater than the corresponding F_2'' values, since the Δ_2F_1'' values appear to be slightly greater,[28] although not surely to an extent beyond experimental error, than the Δ_2F_2'' values.

Initial (^2P) states; comparison of F_1 and F_2 terms. Knowing the F'' values, values of F_1' and F_2' can be determined as illustrated by the following examples (cf. Fig. 2 for justification): $F_{iB}'(2\frac{1}{2}) = R_i(1\frac{1}{2}) + F_i''(1\frac{1}{2})$; $F_{iA}'(2\frac{1}{2}) = Q_i(2\frac{1}{2}) + F_i''(2\frac{1}{2})$, with $i = 1$ or 2. The F'' values can be obtained by calculation from the equation $F_1''(j+1) = F_2''(j) = 5.710 j_k(j_k+1)$, where $j_k = j+\frac{1}{2}$; the use of this equation, for low j values, is probably more accurate than an attempt to determine individual F_1'' and F_2'' values from the experimental data. It is found that the F' values obtained in the manner indicated fulfil the relation $F_{iA}' = F_{iB}'$ within experimental error for *low values* of j. We need therefore here distinguish only F_1' and F_2' levels. Averaging the F' values obtained from P_1, Q_1, and R_1 branches, or from P_2, Q_2, and R_2 branches, the results are as given in Table III; the table can readily be extended to larger j values, if desired. Although too much weight should not be

[28] The Δ_2F_1'' values are to be found in ref. 26, Table II (Part *a*, "low-frequency components"); the Δ_2F_2'' values are given in part *b* of this table ("high-frequency components"), which can be extended to higher m values by using the data of Table I of ref. 26.

attached to the exact figures given, on account of the uncertainty of the calculated F'' values used, the data of Table III show unmistakably that $F_2'(j) > F_1'\ (j+1)$, by an amount which diminishes at first as j increases.

TABLE III. *Initial terms for MgH bands.*

j	$F_2'(j)$	$\Delta_1F_2'(j)$	$F_1'(j+1)$	$\Delta_1F_1'(j+1)$	$F_2'(j)-F_1'(j+1)$
$-\frac{1}{2}$			19,273.28	14.21	
$\frac{1}{2}$			19,287.49	25.03	
$1\frac{1}{2}$	[19,318.0]	[35.3]	19,312.52	36.90	[5.5]
$2\frac{1}{2}$	19,353.34	48.43	19,349.42	48.87	3.92
$3\frac{1}{2}$	19,401.77	60.41	19,398.29	61.04	3.48
$4\frac{1}{2}$	19,462.18	72.64	19,459.33	73.08	2.85
$5\frac{1}{2}$	19,534.82		19,532.41		2.41

(*a*) Lines involving $F_2'(1\frac{1}{2})$ have not yet actually been observed; the values given for this level have been estimated by means of Hill and Van Vleck's formula.

(*b*) The same $F_2'(j)-F_1'(j+1)$ values can also be obtained directly from the doublet separations $P_1(j+1)-P_2(j)$, $Q_1(j+1)-Q_2(j)$, etc.

This involves the assumption $F_2''(j)\sim F_1''(j+1)$, which was also made in calculating Table III. If this holds for high values of j, we may conclude that $F_2'-F_1'$ asymptotically approaches values of about 1.35 and 1.8 for the A and B sub-levels, respectively, since according to Watson and Rudnick,[26] the doublet separations for high j values in the Q branches approach the limiting value 1.35, and in the P and R branches approach the value 1.8.

(*c*) For high values of j, $\Delta F_2'(j)$ and $\Delta F_1'(j+1)$ become asymptotically equal (cf. Δ_2F' values in Table II of ref. 26).

The small, positive, values of $F_2'(j)-F_1'(j+1)$ indicate that the magnetic energy difference in favor of the F_2' term slightly exceeds the kinetic energy difference in favor of the F_1' terms, i.e., we are just on the case a side of the region (cf. discussion in VI, pp. 793–96), typified by the ^2P state of CH, where $F_1 > F_2$. The form of the F''s for MgH (cf. the Δ_1F' values in Table III) does not closely approximate any of the cases of Table I, but the relations $F_2(j) > F_1(j+1)$ and $\Delta F_1(j+1) > \Delta F_2(j) > \Delta F_1(j)$ expected for $^2P_{nab}$ of Table I are fulfilled; the ^2P state of MgH may be said to lie near the $^2P_{nba}$ boundary of $^2P_{nab}$. *At* this boundary ($\Delta E/B = +4$), according to Hill and Van Vleck's formula, the doublets $F_2(j)$, $F_1(j+1)$ should have zero separation for all values of j, the first two F_1 levels, however, not forming doublets. MgH is evidently not far from this case (cf. Fig. 2.). Approximate calculations indicate that the F' values of Table III can be accurately represented by Hill and Van Vleck's formulas[7b] if $\Delta E/B \sim 5.7$ and $B = 6.1$.

Initial (^2P) states: comparison of F_{iA} and F_{iB} terms. As can be seen by a study of Fig. 2, the differences $RQ_i''-QP_i''$ and $RQ_i'-QP_i'$, which represent "combination defects" (cf. Eqs. (1) and (2) for meaning of symbols), should satisfy Eq. (3)

$$RQ_i''-QP_i''=RQ_i'-QP_i'=[F_{iB}'(j+1)+F_{iB}'(j)]-[F_{iA}'(j+1)+F_{iA}(j)] \quad (3)$$

From Table I of ref. 25, it can be seen that for λ5211, $RQ_i''-QP_i''$ is approximately zero up to about $m=10$, then increases to about $+0.8$ for $m=18$ and beyond.[29] Hence, we conclude, $F_{iB}'(j)-F_{iA}'(j)\sim 0.4$ for $m \geqq 18$. This is

[29] The $RQ_1''-QP_1''$ values for λ5622 (Table I of ref. 25), which should agree within experimental error with those for λ5211, since both bands have the same initial states, are *negative* for low values of j. This discrepancy may probably be attributed to errors of measurement.

confirmed by a study of the data in Table I of ref. 26, which also show that $F_{2B}'(m) > F_{2A}'(m)$ by somewhat larger amounts than in the case of F_1'. For low values of j, as we have seen previously, $F_{iA}' = F_{iB}'$ within experimental error.

The CaH Bands

Structure and interpretation. Hulthén[10] has measured and analyzed red CaH bands belonging to two systems, which he designates A and B. In each he has investigated two bands, "A" and "A'," "B" and "B'," which are probably (0,0) and (1,1) bands. The B bands are $^2S \rightarrow {}^2S$. The A system bands each have six branches, and are closely analogous to the green MgH bands, except that the doublets (P_1P_2, etc.) are much more widely separated at low j values, corresponding to a larger $\Delta E/B$. Hulthén shows that for the A band the misssing lines in the P and R branches agree with $F_1'(\frac{1}{2})$ and $F_2'(1\frac{1}{2})$ as the lowest $^2P_{1/2}$ and $^2P_{1\ 1/2}$ levels, respectively; for the A' band the exposure was too weak to detect the lines corresponding to the lowest j values. The first lines of the P_2, Q_2, and R_2 branches, as in MgH, are abnormally weak as compared with the case b theory, but the effect is less marked than in MgH, except perhaps in the Q_2 branch. Hulthén makes no mention of possible satellite branches, but did not make an exhautive study.

Hulthén shows (cf. his Table VI) that the same set of Δ_2F_i'' values is obtainable from the P_i and R_i branches of the A band as from those of the B band ($i = 1$ or 2); similarly for the A' and B' bands. If we agree that the branches which look like P and R really have $\Delta j = \pm 1$, the j' and j'' numberings and F_1 and F_2 designations for both A and B systems now follow, from the specification that j' cannot be less than $\frac{1}{2}$ in the B bands. As shown in V of this series, the resulting assignment for the B bands is in agreement with the intensity theory for $^2S \rightarrow {}^2S$ transitions. The Δ_2F_i' values for the A bands can now be calculated (Hulthén's Table VII). Strictly, these Δ_2F_i' values should be checked by combination relations, such as could be obtained by measuring a (1,0) or (0,1) A band, but from the general theory for $^2P \rightarrow {}^2S$ bands there can be little doubt that they are correct.

From the general theory, Hulthén's Q_1 and Q_2 branches are likewise doubtless correctly designated, but in the absence of data on a (1,0) or (0,1) band, their relation to the other branches is not empirically verified. "Internal" combination relations corresponding to the Eqs. (1) and (2) given above for MgH seem to be not even approximately fulfilled, so that even a probable assignment of j values cannot be made in the Q branches.[30] These difficulties indicate that interesting results would be obtained in

[30] As Hulthén states, the assignment made in his Table II and III is very uncertain. It seems likely that the j numbering in Q_1 should be increased by unity for the A band, but not for the A' band, and that a new first line should be added in the A band, but that the first line given in the A' band should be dropped. Even with these changes, the combination defects are large for the lowest values of j. They decrease for higher values of j, but show irregular variations. Apparently $F_{1A}'(j) - F_{1B}'(j)$ is large for the lowest j values, then decreases. In the Q_2 branches the difficulties are, if anything, worse.

respect to the relation of F_{iA}' and F_{iB}' states if the correct numbering were determined by measurements on a (1,0) or (0,1) band.

Hulthén's designations of the branches and band-lines agree with those used here, except that the j values need to be reduced by $\frac{1}{2}$ unit if they are to agree with the quantum mechanics numbering.

Term values of initial and final states. Taking $F_1''(\frac{1}{2})$ as the zero of energy, the Δ_2F'' values show that $F_i''(j_k)=4.225j_k(j_k+1)\pm 0.0225j_k+\cdots$, with the plus sign for F_1, the minus sign for F_2; j values can be obtained from the relation $j=j_k\pm\frac{1}{2}$. The F'' equation gives the following calculated F'' values: $F_1''(1\frac{1}{2})=8.47$, $F_2''(\frac{1}{2})=8.43$; $F_1''(2\frac{1}{2})=25.39$ (observed, 25.37); $F_2''(1\frac{1}{2})=25.31$, etc. Assuming these calculated values to be correct, F_B' values can be obtained as follows: $F_{1B}'(\frac{1}{2})=P_1(1\frac{1}{2})+F_1''(1\frac{1}{2})$; $F_{1B}'(1\frac{1}{2})=R_1(\frac{1}{2})$; $F_{2B}'(1\frac{1}{2})=R_2(\frac{1}{2})+F_2''(\frac{1}{2})$; $F_{2B}'(2\frac{1}{2})=R_2(1\frac{1}{2})+F_2''(1\frac{1}{2})$; from these by the use of Δ_2F' values from Hulthén's Table VII the F_B''s for higher j's can be built up (the method can be seen by examining, e.g., Fig. 2). Some of the F_B' values so obtained are given in Table IV. On account of the uncertainty as to the j numbering for the Q branches,[30] F_A' values cannot be given with confidence.

TABLE IV. *F_{iB} terms for ^2P state of CaH, from A bands.*

j	$F_2'(j)$	$\Delta_1F_1'(j)$	$F_1'(j+1)$	$\Delta_1F_1'(j+1)$	$F_2'(j)-F_1'(j+1)$
$-\frac{1}{2}$			14,394.35	12.45	
$\frac{1}{2}$			14,406.90	20.74	
$1\frac{1}{2}$	14,479.01	22.54	14,427.64	28.88	51.37
$2\frac{1}{2}$	14,501.55	31.39	14,456.52	36.97	45.03
$3\frac{1}{2}$	14,532.94	40.24	14,493.49	45.18	39.45
$4\frac{1}{2}$	14,573.18		14.538.67		34.51
$18\frac{1}{2}$	16,028.67	164.99	16,027.13	165.95	1.54
$19\frac{1}{2}$	193.66	172.41	193.08	173.81	0.58
$20\frac{1}{2}$	366.07	180.31	366.89	181.23	−0.82
$21\frac{1}{2}$	546.38		548.12		−1.74
$30\frac{1}{2}$	18,495.54	251.08	18,505.53	251.63	−9.99
$31\frac{1}{2}$	746.62	257.41	757.16	258.35	−10.54
$32\frac{1}{2}$	19,004.03	263.69	19,015.51	264.30	−11.48
$33\frac{1}{2}$	267.72		279.81		−12.09

The relations shown in Table IV may be taken as fairly typical of a $^2P_{nab}$ state. For low j values, $\Delta_1F_1(j)\sim\Delta_1F_2(j)$, showing an approach to the case a relation $\Delta_1F_1(j)=\Delta_1F_2(j)$—cf. Table I, $^2P_{na}$. Both Δ_1F's, furthermore, correspond (cf. Table I, especially note 4) to F's of the form $F_i=C_i+B_i^*[j(j+1)]+\cdots$, with $B_1^*=4.09$, $B_2^*=4.49$ for the A band, and with j values which agree with and confirm those assigned above on quite other grounds. Thus, $\Delta_1F_1'(\frac{1}{2})\sim 8.18\times 1\frac{1}{2}$; $\Delta_1F_1'(1\frac{1}{2})\sim 8.18\times 2\frac{1}{2}$, etc., in agreement with the expected relation $\Delta_1F_i(j)\sim 2B_i^*(j+1)$—cf. Table I.

For large j values, $\Delta_1F_2'(j)\sim\Delta_1F_1'(j+1)$, approaching the case b relation (Table I, ^2P_b) $\Delta_1F_2(j)=\Delta_1F_1(j+1)$. But for all values of j, $\Delta_1F_1(j+1)>\Delta_1F_2(j)>\Delta_1F_1(j)$ is fulfilled as expected. Table IV shows the interesting fact that the relation $F_2(j)>F_1(j+1)$ which holds for low j values is reversed beyond $j=19\frac{1}{2}$; possible causes of such a reversal are discussed in Note 6 of

Table I. This reversal corresponds to the fact that $\Delta_1 F_1(j+1)$ remains appreciably greater than $\Delta_1 F_2(j)$ for large j.

The OH Bands

The $^1S \rightarrow {}^2P$ OH bands[31] are the classical example of Heurlinger's "bands with doublet series." They will be considered next because in respect to observed branches and intensity relations—and $|\Delta E/B|$—they constitute an important transition case between the CaH and ZnH bands, although in other respects they fall outside the series of metal hydrides. The fact that the bands are due to OH rather than OH^- or H_2O or H_3O^+ is definitely shown by their doublet character, which shows that their emitter has an odd number of planetary electrons.

Using data of Grebe and Holtz[31] and of Watson,[31] on the (0,0), (1,0), (1,1) and (2,1) bands, Dieke[31] has tested the combination relations and obtained the $\Delta_2 F'$ and $\Delta_2 F''$ values. Assuming only that the obvious Q, R, and P branches really correspond to $\Delta j = 0, \pm 1$, and that the lowest of a set of ^2S levels is always single, Dieke's analysis makes it possible to construct, with assurance of its empirical correctness, the system of energy levels shown in Fig. 3. The missing lines (cf. Table VI) give proof that the lowest levels of each set are as shown.

Final (^2P) states. On comparing the arrangement of the ^2P levels of OH and CaH in Fig. 1, there is at first sight a marked similarity: the levels in each case fall naturally into two sets, one of which begins at a considerable distance above the other. Closer examination discloses an important difference: in OH the nth level of the lower set approaches the nth level of the upper set as j increases, while in CaH the $(n+2)$nd level of the lower set approaches the nth of the upper set. This difference suggested to the writer that the ^2P state is *inverted* in OH (cf. Fig. 1). Kemble[4], and Hill and Van Vleck,[7b] have now shown that the observed behavior in OH is exactly that to be expected theoretically for an inverted ^2P, while the observed relations in CaH (and MgH) correspond to those expected for a normal ^2P state. As will be shown in the last part of this section, j' and j'' values, F_i' and F_i'' designations, and the inverted character of the ^2P state, are now *empirically* assured, assuming only that Δj is limited to $0, \pm 1$, by the discovery[15] of combination relations obeyed by a seventh (non-satellite) branch in the OH bands. This gives valuable support to Kemble's theory, since it can be shown that, in the absence of the new evidence and the theory, an assignment of j values corresponding to a *normal* ^2P state could have been made without contradiction of the rule $\Delta j = 0, \pm 1$ just as well as the assignment corresponding to an inverted ^2P.

[31] L. Grebe and O. Holtz, Ann. der Phys. **39,** 1243 (1912); T. Heurlinger, Dissertation Lund, 1918; R. Fortrat, J. de phys. **5,** 20 (1924); W. W. Watson, Astrophys. J. **60,** 145 (1924); G. H. Dieke, Proc. Acad. Sci. Amsterdam, **28,** 174 (1925); R. T. Birge, Chapter IV, part 5d, of National Research Council Report on Molecular Spectra in Gases; D. Jack, Proc. Roy. Soc. **115***A*, 373 (1927) and **118***A*, 647 (1928); E. C. Kemble, ref. 4.

As Kemble has shown,[4] the form of the Δ_2F'''s (cf. Dieke, l.c.[31]) is approximately that derivable from a term-form $F_i''(j)=B_i^*[j(j+1)-\sigma_i^2]+\cdots$, with $j=1\frac{1}{2}, 2\frac{1}{2}, \cdots$ for the $F_1(^2P_{1\,1/2})$ levels and $j=\frac{1}{2}, 1\frac{1}{2}, \cdots$ for the $F_2(^2P_{1/2})$ levels, and $B_1^*=16.60$, $B_2^*=20.57$. With increasing j, the F_1 levels approach the corresponding F_2 levels but do not pass them as in CaH, at least not in the observed range. Kemble finds in fact that the rate of approach is somewhat *less* than that calculated from his equations, and suggests that this is due to the rotationally induced magnetic field tending here to make $F_2(j)>F_1(j+1)$.[32] A similar effect but with opposite sign may perhaps explain why $F_1(j+1)$ passes $F_2(j)$ in CaH.

TABLE V. *Revised Notation for* OH *Bands.*[a]

New Old[b]	$P_1(1\frac{1}{2})$ $P_2(2)$	$Q_1(1\frac{1}{2})$ $Q_2(2)$	$Q_1A_1B(1\frac{1}{2})$ $\sigma Q_2(2)$ of Watson		${}^QP_{21}(1\frac{1}{2})$ $F_1(2)-f_2'(\frac{1}{2})$ *Sat.*$Q_2(2)$	$R_1(1\frac{1}{2})$ $R_2(2)$	${}^RQ_{21}(1\frac{1}{2})$ $\sigma R_2(2)$ *Sat* $R_2(2)$	${}^{RR}R_{21}(1\frac{1}{2})$ (Previously undesignated)
New Old[b]	${}^{PP}P_{12}(1\frac{1}{2})$ (Unknown)	$P_2(1\frac{1}{2})$ $P_1(3)$	${}^PQ_{12}(\frac{1}{2})$ $P_1(2)$	${}^PQ_{12}(1\frac{1}{2})$ $\sigma P_1(3)$ or Sat. $P_1(3)$	$Q_2(\frac{1}{2})$ $Q_1(2)$	$Q_2A_2B(\frac{1}{2})$ $\sigma Q_1(2)$ of Watson	${}^QR_{12}(\frac{1}{2})$ Sat. $Q_1(2)$	$R_2(\frac{1}{2})$ $R_1(2)$
New Old[b,c]	$F_1'(\frac{1}{2})$ $F_2(1)$	$F_2'(\frac{1}{2})$ $F_1(2)$	$F_1A''(1\frac{1}{2})$ $f_2'(2)$	$F_1B''(1\frac{1}{2})$ $f_2(2)$	$F_2A''(\frac{1}{2})$ $f_1'(2)$	$F_2B''(\frac{1}{2})$ $f_2'(2)$		

Notes. (*a*) The j'' numbers given correspond to the *predicted* first line in each branch, but are not intended to imply that this line has been recorded in the case of every branch.

(*b*) The old notation and (*m*) numbering originated with Heurlinger. Satellite notation has been used with varying degrees of explicitness by Heurlinger, Fortrat, Dieke and Watson.[31]

(*c*) The old F, f, f' term notation is that given by Dieke. Dieke's supposed state $F_1(2)$, involved in his line $P_1(2)$, is really identical, according to the present interpretation, with his $F_2(1)$.

TABLE VI. *Predicted and observed j'' values for first lines in* OH *branches.*

Branch	(2, 0) *band*	(1, 0) *band*	(2, 1) *band*	(0, 0) *band*	(0, 1) *band*	*Predicted j''*
P_1	$1\frac{1}{2}$	$1\frac{1}{2}$	$1\frac{1}{2}$	$1\frac{1}{2}$	$1\frac{1}{2}$	$1\frac{1}{2}$
Q_1	$1\frac{1}{2}$	$(1\frac{1}{2})$	$1\frac{1}{2}$	$(1\frac{1}{2})$	$1\frac{1}{2}$	$1\frac{1}{2}$
R_1	$1\frac{1}{2}$	$1\frac{1}{2}$	$3\frac{1}{2}$	$1\frac{1}{2}$	$1\frac{1}{2}$	$1\frac{1}{2}$
P_2	$(1\frac{1}{2})$	$(1\frac{1}{2})$	$1\frac{1}{2}$	$1\frac{1}{2}$	$1\frac{1}{2}$	$1\frac{1}{2}$
${}^PQ_{12}$	$\frac{1}{2}$	$(\frac{1}{2})$	$\frac{1}{2}$	$\frac{1}{2}$	$\frac{1}{2}$	$\frac{1}{2}$
Q_2	$(\frac{1}{2})$	$(\frac{1}{2})$	$\frac{1}{2}$	$\frac{1}{2}$	$\frac{1}{2}$	$\frac{1}{2}$
R_2	$(\frac{1}{2})$	$\frac{1}{2}$	$2\frac{1}{2}$	$\frac{1}{2}$	$\frac{1}{2}$	$\frac{1}{2}$
${}^{RR}R_{21}$	–	$1\frac{1}{2}$	–	$1\frac{1}{2}$	–	$1\frac{1}{2}$

Notes. (1, 0) and (2, 1) bands (λ2811), data of Watson[31]; (0, 0) band (λ3064), data of Grebe and Holtz[31]; (2, 0) and (0, 1) bands (λλ2608 and 3428), data of Jack.[31] Values given in parenthesis are inconclusive because of superposition of other lines. The apparent disagreement in the R branches of the (2, 1) band is doubtless a result of the weakness of these branches (cf. Table VIII).

Notation. The interpretation of the OH bands given by Kemble and the writer necessitates a *reversal of the subscripts 1 and 2*, as compared with the designations introduced by Heurlinger, in order to bring the notation into

[32] This effect is probably even greater than appears in Kemble's Fig. 4, since the empirical curves in his Fig. 4 are based on the use of his Eq. (43), which assumes that the F' doublet separations, in the ^2S initial state (cf. Eq. (4) above), are negligible.

harmony with the scheme proposed in VI. The change seems desirable, in spite of temporary confusion which may result, because it makes possible uniform designations for analogous branches in all spectra corresponding to the same type of electron jump. Table V shows the old and new notation for the OH bands.

Term values for initial (^2S) *states.* For the initial states, Dieke's Table II[31] shows unquestionably that (in the present notation, which is the reverse of Dieke's—cf. Table V), $\Delta_2F_1' > \Delta_2F_2'$ from the beginning. Hence, assuming in accordance with the theory for ^2S states that the lowest ^2S state is the single level $F_1'(\frac{1}{2})$, the relation $F_1'(j+1) > F_2'(j)$ holds. The quantitative relation for the rotational energy, for the vibrational state $n'=0$, is approximately

$$F'(j_k) = 16.85[j_k(j_k+1)] \pm 0.11 j_k \tag{4}$$

This gives for $F_1(j_k) - F_2(j_k)$, for $j_k = 1, 2, 3, \cdots$ the calculated values 0.22, 0.44, 0.66, $\cdots$.

Comparison of F_{iA}'' *and* F_{iB}'' *terms* (σ-*type doubling in* ^2P *states*). From Fig. 3 it will be seen that the following relations should hold:

$$[R_i(j) - Q_i(j+1)] - [Q_i(j) - P_i(j+1)] = [F_{iA}''(j) + F_{iA}''(j+1)] - [F_{iB}''(j) + F_{iB}''(j+1)] \cong 2[F_{iA}''(j+\tfrac{1}{2}) - F_{iB}''(j+\tfrac{1}{2})] = 2\delta_{AB}F_i''(j+\tfrac{1}{2}) \tag{5}$$

The last equality in Eq. (5) merely *defines* the quantity $\delta_{AB}F_i(j)$.

While this method does not give exact individual values of the doublet intervals, it should give a good idea of the mode of variation of σ-type doublet separations as a function of j. Values of $\delta_{AB}F_i''(j)$ could also be obtained directly from data on Q_i branches and their $Q_{iA\,iB}$ satellites (see later section) by means of the relation:

$$\delta_{AB}F_i''(j) = Q_{iA\,iB}(j) - Q_i(j). \tag{6}$$

TABLE VII. *Doublet intervals in* σ-*type doubling for* ^2P *levels in OH.*

$j+\frac{1}{2}$	$\delta_{AB}F_1''(j+\frac{1}{2})$	$\delta_{AB}F_2''(j+\frac{1}{2})$	$j+\frac{1}{2}$	$\delta_{AB}F_1''(j+\frac{1}{2})$	$\delta_{AB}F_2''(j+\frac{1}{2})$
1		−0.11	11	+5.10	+3.40
2	+0.12	−0.18	12	+6.15	4.11
3	0.31	−0.19	13	7.03	4.66
4	0.56	−0.06	14	7.74	5.50
5	0.98	+0.21	15	8.94	6.53
6	1.35	+0.49	16	10.03	7.31
7	2.12	0.79	17	11.24	8.34
8	2.69	1.28	18	12.26	9.44
9	3.45	1.85	19	13.36	10.31
10	4.28	2.52	20	14.52	11.49
			21	15.93	

Note. The above values were obtained from Dieke's Table I as follows: the subtraction $[R_1'(m) - Q_1'(m+1)] - [Q_1'(m) - P_1'(m+1)]$, in Dieke's notation, was performed for λ3064 and for λ2811, and the average of these results was taken as $2\delta_{AB}F_2''(j+\frac{1}{2})$, with $j+\frac{1}{2} = m-1$ (cf. Table V for key to changes of notation). Similarly, an average value of $2\delta_{AB}F_1''(j+\frac{1}{2})$ was obtained from $[R_2'(m) - Q_2'(m+1)] - [Q_2'(m) - P_2'(m+1)$, with $j+\frac{1}{2} = m$ in this case. Division of each result by two gave the values listed above.

But the less direct method of Eq. (5) seems preferable, because the data available for use in Eq. (6) are not very satisfactory.

Table I of Dieke's paper gives differences of the type R-Q, Q-P, etc., required for use in Eq. (5). Using Dieke's values and performing the necessary subtractions, the results given in Table VII are obtained. The different behavior of the F_1'' and F_2'' levels, and the reversal of sign for low values of j in the F_2 levels, are noteworthy. The data on MgH show indications of similar behavior, except that the rôles of the F_1 and F_2 levels appear to be interchanged, and that the observed effects are much smaller.

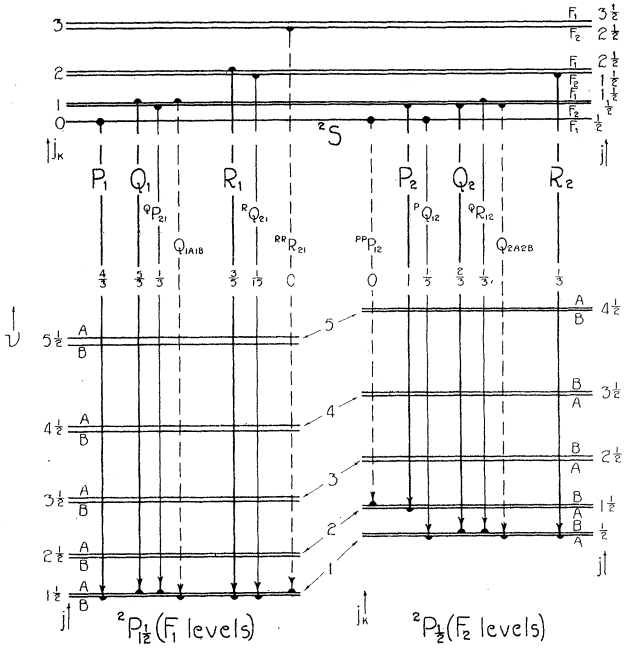

Fig. 3. *Lowest rotational levels of each electronic state, and first line of each branch, with its theoretical intensity as calculated for case b from Eqs.* (14)-(22) *of* VI, *for* OH λ2811 (1, 0 *band*). The rotational levels are drawn to scale, making use of the ΔF data of Dieke,[31] except that all doublet separations are exaggerated (cf. Table VII for numerical data on ^2P level doubling). The strong full vertical lines represent main branches, the weak full vertical lines, normal satellite branches. Two of the broken vertical lines represent branches which would be forbidden in case b: of these $^{RR}R_{21}$ is known, but $^{PP}P_{12}$ is not yet known. The other two broken lines represent weak satellite branches which violate the ordinary selection rules of σ-type doubling. The j_k values given for the ^2P state are those which would be appropriate in case b, although for the lowest rotational levels in OH, which are near case a, they have little real meaning.

Intensity relations and first lines. Intensities predicted by the equations[2] corresponding to Hund's case b, for the first line of each of the various main and satellite branches, are given in Fig. 3. The observed first lines, including the satellite line $^PQ_{12}(\frac{1}{2})$, are within the errors of determination exactly as predicted (cf. Table VI). Both predicted intensities and first lines, incidentally, are the same as in CH λ3900.

Some of the observed intensities recorded by Watson and Jack for four of the OH bands are given in Table VIII. The major intensity relation $Q>P>R$ characteristic of $S\rightarrow P$ transitions (cf. III, IV, and VI of this series) is obviously fulfilled. Another predicted relation for case b (cf. Eqs. (14)–(22) of VI) is that for small values of j, $R_1>R_2$, $Q_1>Q_2$, $P_1>P_2$ for the members of each doublet, with asymptotic equality of intensity of doublet components for large j. These relations are on the whole fulfilled, but there is evidence that the inequalities for low j are more pronounced than expected in the case of the R branches, but are less pronounced than expected, or even reversed, in the P branches. The satellite branches (see below) show unpredicted relatively high intensity. Also, an additional R branch is present which should not appear at all in case b. These various departures from the case b intensity relations may be attributed to the fact that the ^2P state is well on the way toward case a. The observed agreement is on the whole surprisingly good.

TABLE VIII. *Observed intensity relations in OH bands.*

$j-\frac{1}{2}$	$R_1(j+1)$	$R_2(j)$	$Q_1(j+1)$	$Q_2(j)$	$P_1(j+1)$	$P_2(j)$	$R_1(j+1)$	$R_2(j)$	$Q_1(j+1)$	$Q_2(j)$	$P_1(j+1)$	$P_2(j)$
	λ2811 (1, 0) band (data of Watson[31])						λ2875 (2, 1) band (data of Watson[31])					
0	3	0	*	*	5	*	–	–	7	2	2	0
1	4	2	9	5	5	*	–	–	9	5	5	5
2	4	*	9	6	6	9	*	0	*	4	*	*
3	4	4	10	7	8	9	*	4	8	8	*	7
4	*	4	10	*	8	9	6	*	*	8	7	8
5	*	*	*	10	9	9	*	0	8	*	*	8
6	4	*	10	10	9	8	*	*	8	*	7	6
	λ2608 (2, 0) band (data of Jack[31])						λ3428 (0, 1) band (data of Jack[31])					
0	6	*	8	*	5	*	6	0	7	5	1	5
1	7	3	10	*	9	8	2	*	6	8	9	5
2	8	4	9	8	8	9	5	1	7	9	5	8
3	7	5	10	*	9	9	3	2	7	9	5	8
4	6	8	9	9	9	9	2	2	7	8	6	5
5	7	5	10	9	9	7	0	5	7	5	5	*
6	4	*	*	9	8	7	10	10	9	5	2	*

Note. Data for higher values of j can be found in Watson's and Jack's papers.

Satellite series. The satellite branches in OH, first noted by Heurlinger and later extensively investigated by Fortrat, have been shown by Dieke to correspond to combinations (cf. Fig. 3) between the same levels which are needed to explain the main branches (cf. Table VI for Dieke's notation). It is only because of their abnormally high intensity, and because of the comparatively large $F_1'-F_2'$ values in the ^2S state (cf. Eq. (4), which permit resolution of the satellite from the corresponding main lines, that it is possible to establish the existence of the satellite series.[32a] This was not possible for CH λ3900 or MgH, for both of which $F_1(j+1)-F_2(j)$ for the ^2S state is small even for large j.

[32a] This statement is not intended to apply to the abnormal satellite series (see below) which violate the selection rules of σ-type doubling.

For the P and R branches, the satellites are exactly those expected: R_2 and P_1 have no satellite series, R_1 and P_2 each have one, according to Fortrat's data on the λ3064(0,0) band (*l.c.*,[31] Tables II and IV). The recorded lines of the P_2 satellite series in ${}^{P}Q_{12}$ extend from $j''=2\frac{1}{2}$ to $j''=12\frac{1}{2}$. According to Fortrat (*l.c.*,[31] top p. 23) ${}^{P}Q_{12}(2\frac{1}{2})$ is of equal intensity with the corresponding main line $P_2(2\frac{1}{2})$. Successive satellite lines show increasing intensity,[33] but with a less rapid increase than in the main branch, followed by falling intensity beyond ${}^{P}Q_{12}(6\frac{1}{2})$; the last satellite line detected was ${}^{P}Q_{12}(12\frac{1}{2})$, while the main branch was followed to $P_2(26\frac{1}{2})$. The intensities in the ${}^{P}Q_{12}$ branch are evidently much greater than those predicted for case b (cf. VI, Eq. (19), and Fig. 3 of VII), but they nevertheless still show a marked tendency toward the predicted case b behavior of falling off inversely as j_k.—According to the present interpretation, the previously supposed first line of the P_1 branch is really ${}^{P}Q_{12}(\frac{1}{2})$, there being no corresponding main line. The apparent absence of ${}^{P}Q_{21}(1\frac{1}{2})$ is evidently due merely to a lack of resolution from the corresponding main line $P_1(1\frac{1}{2})$; the calculated separation is 0.26 wave numbers.—In the ${}^{R}Q_{21}$ branch (satellite of R_2), the recorded lines extend from $j''=1\frac{1}{2}$ to $j''=4\frac{1}{2}$,[34] with recorded intensities falling from 3 to 1; the predicted first line ${}^{R}Q_{21}(\frac{1}{2})$ falls on an R_2 line.

Each of the Q branches is accompanied by more than one satellite series. In the case of the Q_2 branch, satellite lines of the expected type (${}^{Q}R_{12}$) appear to be present up to $j''=11\frac{1}{2}$ or $12\frac{1}{2}$. In the Q_1 branch, the expected satellites (${}^{Q}P_{21}$) extend to at least $j''=6\frac{1}{2}$. In both cases, the intensity rises to a maximum for a low value of j, then falls (cf. Fortrat, *l. c.*, p. 26–7).

In addition, as Dieke[31] and Watson[35] have shown, there are Q satellite branches which in the present notation (cf. VI) are Q_{2A2B} and Q_{1A1B}. These branches, unlike the other satellites, extend to fairly large j values, i.e., the intensity distribution as a function of j is similar to that in the main branches. They constitute the only known cases where the σ-type doubling selection rules for Q branches ($A\rightarrow A$ or $B\rightarrow B$), which also hold for ${}^{Q}P$ and ${}^{Q}R$ branches, and which are probably associated with $\Delta j_k=0$, rather than with $\Delta j=0$, are broken through.

The satellite series given above do not exhaust Fortrat's data; especially in the Q_1 branch (Q_2 of Fortrat) there are many additional unexplained satellite lines. Dieke has concluded that some of these belong to a ${}^{Q}P_{2A1B}$ branch (combination F_1-f_2 in Dieke's notation), but a recalculation of the expected positions from Eq. (4) and Table VII seems not to justify this conclusion. Further, ${}^{Q}P_{2A1B}$ would hardly be expected in measurable intensity, since it bears to the already weak satellite branch ${}^{Q}P_{21}$ the same relation as the weak branch Q_{1A1B} to the strong branch Q_1. One might,

[33] Fortrat's statement to this effect seems to be partially contradicted by his recorded intensities (Table II), which are, beginning with Q_{12} ($2\frac{1}{2}$), 3, 3, 2,—, 2, 1,—, 1, 1, 1, 0.

[34] Additional lines up to $j''=8\frac{1}{2}$, recorded by Fortrat, fail to fulfill the proper combination relations.

[35] W. W. Watson, Nature, Jan. 30, 1926: new measurements on Q_{1A1B} and Q_{2A2B}.

however, expect to find additional weak branches, violating the σ-type doubling selection rules, as satellites of the strong P and R branches.

Identification of seventh non-satellite branch in OH *bands.* Watson has given data[31] on a previously undescribed weak series of lines associated with the λ3064 OH band. This series starts near the λ3064 head, and extends to λ3021 where it forms an additional head. Jack has subsequently found and measured an analogous branch in the λ2811 band.

It is natural to suppose that this very weak head is analogous to one of the outlying heads in the four-headed type of $^2S\rightarrow{}^2P$ or $^2P\rightarrow{}^2S$ bands of which the NO γ and the BO α bands are examples. In such bands, one of the four heads is formed either by the $^{PP}P_{12}$ or by the $^{RR}R_{21}$ branch, both of which should be absent for a case b ^2P state. Since the intensity relations in the OH bands are close to those of case b, such branches should be very weak, but in view of the strength of the satellite series (cf. above), they might well be of detectable intensity. We shall then assume that the OH branch in question is an $^{RR}R_{21}$ branch, and proceed to test the correctness of this assumption by means of combination relations.

From Fig. 3 it will be seen that the following relations should hold:

$$^{RR}R_{21}(j)=F_2'(j+1)-F_{1A}''(j)=[F_2'(j-1)-F_{1A}''(i)]$$
$$+[F_2'(j+1)-F_2'(j-1)]={}^{Q}P_{21}(j)+\Delta_2F_2'(j) \qquad (7)$$

From experimental data on the $^{Q}P_{21}$ lines and on the Δ_2F_2' values, we should be able to predict the positions of the $^{RR}R_{21}$ lines. The $^{Q}P_{21}$ branch is, however, unfortunately a weak satellite branch, for which the data are fragmentary and uncertain. By making a slight use of the theory, we can, however, calculate the positions of the $^{Q}P_{21}$ lines fairly accurately from data on the corresponding main branch (Q_1) together with estimated values of $[F_1'(j)-F_2'(j-1)]$; according to Fig. 3 and Eq. (4)—noting that $j=j_k\pm\frac{1}{2}$ in Eq. (4)—we have

$$^{Q}P_{21}(j)=Q_1(j)-[F_1'(j)-F_2'(j-1)]=Q_1(j)-0.22(j-\tfrac{1}{2}). \qquad (8)$$

Hence we expect with considerable accuracy

$$^{RR}R_{21}(j)=Q_1(j)+\Delta_2F_2'(j)-0.22\ (j-\tfrac{1}{2}) \qquad (9)$$

The value 0.22, from Eq. (4), refers to the state $n'=0$, and so is applicable to the prediction of the $^{RR}R_{21}$ series for the λ3064(0,0) band. For the λ2811(1,0) band, a corresponding value for the state $n'=1$ should be used. There are, however, so many superpositions of lines in Watson's data on the λ2811 band that no accurate estimate of this coefficient can be made, and we shall merely assume that the same value is applicable for $n'=1$ as for $n'=0$.

Table IX shows that the positions of the observed lines of the $^{RR}R_{21}$ branch are in satisfactory agreement with the calculated positions, thus confirming our assumption. The small differences between observed and

calculated values are not surprising, since the observed and calculated values involve data of different observers, and since the assumption $F_1'(j) - F_2'(j-1) = 0.22(j-\frac{1}{2})$ is not known to be more than approximately true.

TABLE IX. *Calculated and observed positions of lines of* $^{RR}R_{21}$ *branch. (calculations according to Eq.(9))*

	λ3064 (0, 0) *band*			λ2811 (1, 0) *band*		
$j+\frac{1}{2}$	Calc'd ν	Obs'd ν (Watson)	Int.	Calc'd ν	Obs'd ν (Jack)	Int.
2	32,643.42	32,643.39	8	35,622.08*	35,621.67	10
3	694.45	694.52	8	666.46*	666.65	10
4	745.10	744.61	7	708.32	708.29	10
5	793.07	792.80	6	746.80	746.59	10
6	838.62	838.44	5	780.93*	780.48	9
7	881.60*	881.18	4	809.98*	809.82	8
8	920.76*	920.61	4	834.37	834.20	7
9	956.68	956.57	3	853.35*	853.60	6
10	988.58	988.47	2	867.25	867.36	5
11	33,016.68	33,016.53	1	875.24	876.63?	—
12	040.14	040.11	0	877.15*	876.63	4
13	059.36	059.16	–	872.98*	873.28	4
14	074.10	073.54–	–	863.24*	862.60	3
15	083.90	083.79	0–	847.11*	846.41*	2*
16	089.00			823.00	823.16*	1*
17	088.94	088.92	1*d*	793.26	793.16*	1*
18	083.85	083.79	–	756.17	756.56*	0*
19	073.09	073.54–				
20	056.92					

Notes. The data used in the calculations are from the following sources: λ3064 band, Q_1 data from Fortrat, Δ_2F_2' values as given by Dieke (cf. his Table II), from data of Grebe and Holtz; λ2811 band, Q_1 data from Watson, Δ_2F_2' values as given by Dieke (Table II) from data of Watson. For the convenience of the reader in case he desires to refer to these data, it may be noted that in terms of the old notation $Q_1(j)$ of Eq. (9) becomes $Q_2(m)$ of Fortrat or $Q_2'(m)$ of Watson, with $m=j+\frac{1}{2}$, while $\Delta_2F_2'(j)$ becomes $\Delta F_1(m-1)$ of Dieke, with $m-1=j+\frac{1}{2}$. The observed wave-numbers for the R_{21} branch are from Watson, *l.c.*,[31] p. 158, for λ3064; Jack, 1927 paper,[31] p. 389, for λ2811. The intensities given have only *relative* significance, and this only within each band.

It will be noted (cf. Table IX) that each $^{RR}R_{21}$ branch begins, as expected (cf. Fig. 3), with $^{RR}R_{21}(1\frac{1}{2})$. According to the data in Table IX, the intensity reaches a maximum at about the second line, then falls off steadily. This is in accordance with the fact that this branch corresponds to a strong transition for a case *a* ^2P state (cf. HgH) but to a forbidden transition for a case *b* ^2P state; for the lowest values of j, the ^2P state is close to case *a*, but steadily approaches case *b* as j increases. It is of interest to note that the phenomenon of an early intensity maximum followed by rapid falling off is more pronounced here than in the legitimate satellite branches (cf. above); this difference is probably correlated with the fact that the satellite branches are merely very weak but not forbidden in case *b*.

In view of the presence of a weak $^{RR}R_{21}$ branch in the OH bands, the presence of a weak $^{PP}P_{12}$ branch may be predicted. This should perhaps be stronger than the R_{21} branch, but must be less favorably situated for observation, since it should be in the midst of the strong branches, while the R_{21} branch occupies an isolated position (cf. reproduction in Jack's 1927 paper[31]).

ZnH, CdH, and HgH Bands

Interpretation. The interpretation of the ZnH, CdH, and HgH bands has been discussed previously by Hulthén, Kratzer,[36] and the writer.[37] The interpretation given previously by the writer assumed what would now be called a $^2P_{na}$ initial and a ^2S final state.

The ^2P terms were written in the form $F_1',_2(^2P_i) = B_i[(j^2-\sigma_i^2)^{1/2} \mp \epsilon]^2 + \cdots$, with $\sigma_i \sim \frac{1}{2}$ or $1\frac{1}{2}$ for $^2P_{1/2}$ or $^2P_{1\ 1/2}$, and with $\mp\epsilon$ corresponding to F_1' and F_2'. The use of $\mp\epsilon$ implied ρ-type doubling like that of the ^2S state, but we must now of course interpret it as σ-type doubling. The term-form (cf. following paragraph in regard to data on term values) may now perhaps

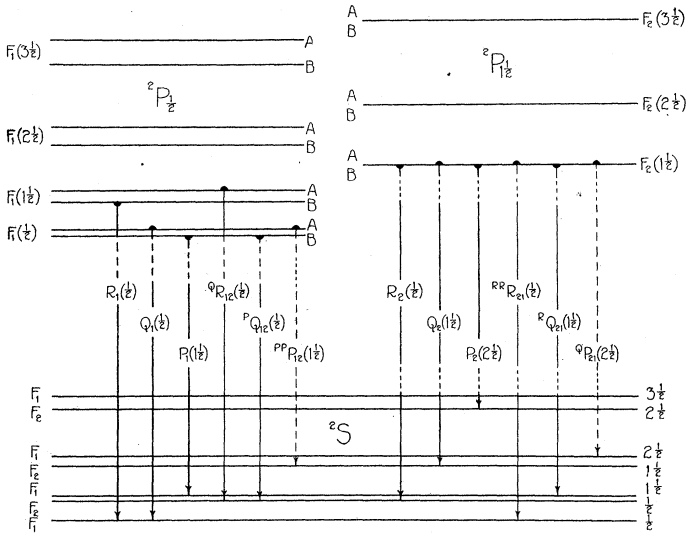

Fig. 4. *Lowest rotational levels, and first lines of each branch, for HgH* (0, 0) *bands* λ3500 ($^2P_{1\frac{1}{2}} \rightarrow {}^2S$ *sub-band*) *and* λ4017 ($^2P_{\frac{1}{2}} \rightarrow {}^2S$ *sub-band*). The $^2P_{1\frac{1}{2}}$, $^2P_{\frac{1}{2}}$, and ^2S sets of levels are all drawn to the same scale from Hulthén's data (cf. paragraph in the text on "Term Values of HgH)." Because of space limitations, however, the $^2P_{1\frac{1}{2}}$ and $^2P_{\frac{1}{2}}$ sets of levels could not be drawn in their true relative positions; the $^2P_{1\frac{1}{2}}$ levels shown are actually all much higher than the $^2P_{\frac{1}{2}}$ levels shown. Strong vertical lines, weak vertical lines, a nd dashed vertical lines respectively indicate branches which in case *b* would be main, satellite, and forbidden branches. *All* these branches are strong in HgH.

best be expressed for low values of j as $F_{i\alpha}'(j) = B_i^*[j(j+1)-\sigma_i^2] \pm \delta j + \cdots$, where $i=1$ or 2 and $\alpha = A$ or B, with $\sigma_1 = \frac{1}{2}$ (F_1 or $^2P_{1/2}$ terms) and $\sigma_2 = 1\frac{1}{2}$ (F_2 or $^2P_{1\ 1/2}$ terms); $+\delta j$ goes with $\alpha = A$, $-\delta j$ with $\alpha = B$, hence $F_A(j) > F_B(j)$: cf. Fig. 4. In this formula, δ is practically zero[38] for the $^2P_{1\ 1/2}$ states for all three molecules; but for the $^2P_{1/2}$ states $\delta \sim 0.02\ B_1^*$ for ZnH, $0.06\ B_1^*$ for CdH, and $0.19\ B_1^*$ for HgH, corresponding to a large-scale σ-type

[36] A. Kratzer, Ann. der Physik, **71,** 89 (1923).

[37] R. S. Mulliken, Proc. Nat. Acad. Sci. **12,** 151 (1926); also E. Hulthén, ref. 14.

[38] The existence of any doubling at all in the F_2 states is shown only in the case of certain perturbed lines in HgH (cf. E. Hulthén, Zeits. f. Physik **32,** 32. 1925, and H. Ludloff, Zeits. f. Physik, **34,** 485, 1925).

doubling, especially in HgH. It is hardly necessary to say that the difference between B_1* and B_2*, previously interpreted as caused by a real difference in moments of inertia, is now to be explained by Kemble's theory.

Term values of HgH. Hulthén in his 1925 paper has given a complete list of term values for HgH, for both ^2S states (cf. his Table 8) and ^2P states (cf. his Table 7: his $n=0$ and $n=1$ belong to the $^2P_{1/2}$, his $n'=0$ and 1 to the $^2P_{1\ 1/2}$ terms). His term values are based on the assumption $F_1(\frac{1}{2})=9.8$ for the lowest ^2S level and should all be lowered by 9.8 if one wishes to take $F_1(\frac{1}{2})$ as the zero of energy, as is natural in the present state of the theory. At the end of Table X is given a key for translating Hulthén's notation into that used here.

The arrangement of the energy levels, and their relation to the observed branches, are shown for HgH in Fig. 4.

Notation. A revised notation for the ZnH, CdH, and HgH bands, in harmony with that proposed in VI, is given in Table X, together with earlier notations of various authors. It is to be hoped that no further changes will be needed.

TABLE X. *New and old notations for first line of each branch in* ZnH, CdH, *and* HgH *bands*

Present	$R_1(\frac{1}{2})$	$^QR_{12}(\frac{1}{2})$	$Q_1(\frac{1}{2})$	$^PQ_{12}(\frac{1}{2})$	$P_1(1\frac{1}{2})$	$^{PP}P_{12}(1\frac{1}{2})$	
Birge[31] 1927	$R^-(1)$	$R^+(1)$	$Q^\mp(1)$	$Q^\pm(1)$	$P^-(2)$	$P^+(2)$	
Mulliken[37] 1926	R_1	R_2	Q_1	Q_2	P_1	P_2	$^2P_{1/2}\rightarrow S^2$
Hulthén[39] 1923–5	R_2	R_1	Q_2	Q_1	P_2	P_1	
Kratzer[36] 1923	R_1	R_2	Q_2	Q_1	P_1	P_2	
Hulthén 1922	R_1	R_2	R_3	P_3	P_2	P_1	
Present	$^{RR}R_{21}(\frac{1}{2})$	$R_2(\frac{1}{2})$	$^RQ_{21}(1\frac{1}{2})$	$Q_2(1\frac{1}{2})$	$^QP_{21}(2\frac{1}{2})$	$P_2(2\frac{1}{2})$	
Birge[31] 1927	$R^-(1)$	$R^+(1)$	$Q^\pm(2)$	$Q^\mp(2)$	$P^-(3)$	$P^+(3)$	
Mulliken[37] 1926	R_1	R_2	Q_1	Q_2	P_1	P_2	$P_{1\ 1/2}\rightarrow ^2S$
Hulthén[39] 1923–5	R_2	R_1	Q_2	Q_1	P_2	P_1	
Kratzer[36] 1923	R_1	R_2	Q_1	Q_1	P_1	P_2	
Hulthén 1922	R_1	R_2	R_3	P_3	P_2	P_1	

Notes. (a) In regard to the earliest series notation, that of Liese, cf. Hulthén, Diss. Lund 1923, p. 34.

(b) The numbers in parentheses are the same for all the old notations as for that of Birge, and so have not been repeated.

	^2P *levels*			^2S levels	
Present	$F_{iA}(\frac{1}{2})$	$F_{iB}(\frac{1}{2})$	$F_2(1\frac{1}{2})$	$F_1(\frac{1}{2})$	$F_2(\frac{1}{2})$
Hulthén 1925	$F_1(1)$	$F_2(1)$	$F(2)$	$F_2(1)$	$F_1(1)$

Note. Hulthén's notation is that used in his Tables 7 and 8 of ref. 39 (1925 paper); cf. paragraph on "Term Values" above.

Intensity relations. As already noted in the first section of this paper, the satellite and forbidden branches of case *b* show a progressive increase in intensity in the series ZnH, CdH, and HgH, until in HgH all branches are about equally strong, according to data of Hulthén.[39] This last result is in

[39] E. Hulthén, Dissertation Lund 1923, and Zeits. f. Physik **32**, 32, 1925. In HgH the $^2P_{1\frac{1}{2}}\rightarrow ^2S$ branches as a whole are much weaker (Hulthén, cf. footnote 9 of ref. 37) than the $^2P_{\frac{1}{2}}\rightarrow ^2S$ branches, but this effect may be attributed to the conditions of excitation: the $^2P_{\frac{1}{2}}$ levels as a whole might naturally be more readily excited than the much higher-lying $^2P_{1\frac{1}{2}}$ levels.

complete agreement with the theory of Hill and Van Vleck. ZnH is an interesting transition case. Here in the orthodox branches P_i, Q_i, and R_i the major intensity relation $Q>R>P$ characteristic of a $P\rightarrow S$ transition is found.[40] Similar relations exist in the unorthodox branches, which are, however, on the whole, only about half as intense as the orthodox. An interesting point is that the unorthodox branches reach a maximum intensity at a much smaller value of j than the orthodox branches. This is to be explained by the fact that for large values of j case b is being approached. A similar phenomenon is noted in the OH bands (cf. above).

NO Bands

NO γ *bands.* The NO γ bands, whose structure (eight branches) has been analyzed by Guillery,[41] show the features expected for a $^2S\rightarrow{}^2P_{nab}$ transition in which the doublets $F_1(j+1)$ and $F_2(j)$ of the ^2S levels are (within the experimental accuracy) unresolved. Table XI shows the relation of Guillery's notation to the present notation, and Fig. 5 shows the relations which exist between rotational levels and observed branches.

TABLE XI. *Revised notation and predicted first lines for NO γ bands.*

Present	$P_1(1\frac{1}{2})$	$Q_1(\frac{1}{2})$	$Q_1(1\frac{1}{2})+{}^QP_{21}(1\frac{1}{2})$	$R_1(\frac{1}{2})+{}^RQ_{21}(\frac{1}{2})$	${}^{RR}R_{21}(\frac{1}{2})$	$\}{}^2S\rightarrow{}^2P_{1/2}$
Guillery	$P_2(1)$	$Q_2(1)$	$Q_2(2)$	$R_2(2)$	$R_2'(3)$	
Present	${}^{PP}P_{12}(1\frac{1}{2})$	$P_2(1\frac{1}{2})+{}^PQ_{12}(1\frac{1}{2})$		$Q_2(1\frac{1}{2})+{}^QR_{12}(1\frac{1}{2})$	$R_2(1\frac{1}{2})$	$\}{}^2S\rightarrow{}^2P_{1\,1/2}$
Guillery	$P_1(1)$	$Q_1(2)$		$R_1(3)$	$R_1'(4)$	

Since for the lower ^2P state of NO, the value of $\Delta E/B$ is near that in ZnH (cf. Table II), we may expect similar intensity relations. The observed relations[41] may be summarized as follows: $[Q_2+{}^QR_{12}]>[Q_1+{}^QP_{21}]>[R_1+{}^RQ_{21}]>[P_2+{}^PQ_{12}]\sim P_1>>{}^{PP}P_{12}>R_2>{}^{RR}R_{21}$. Because of the coalescence of the satellite branches with corresponding main branches, the individual intensities cannot be determined in all cases, but the comparatively low intensity of the unorthodox ${}^{PP}P_{12}$ and ${}^{RR}R_{21}$ branches is evident. The observed intensities appear also to agree with the general relation $Q>P>R$ expected for an $S\rightarrow P$ transition. The rather surprising contrast $R_2<<R_1$ which apparently exists finds to some extent a parallel in the OH bands (cf. Table VIII) and elsewhere.

So far as can be judged from the data,[41] the observed first lines in the various branches are in reasonable agreement, taking into consideration the experimental difficulties, with those predicted in Table XI. In several cases one or two unpredicted lines are assigned by Guillery at the beginning of a branch, but in nearly all such instances, the lines in question are lines which also fit in other series.

[40] E. Hulthén, Diss. Lund, 1923, p. 26.

[41] M. Guillery, Zeits. f. Physik, **42,** 121 (1927).

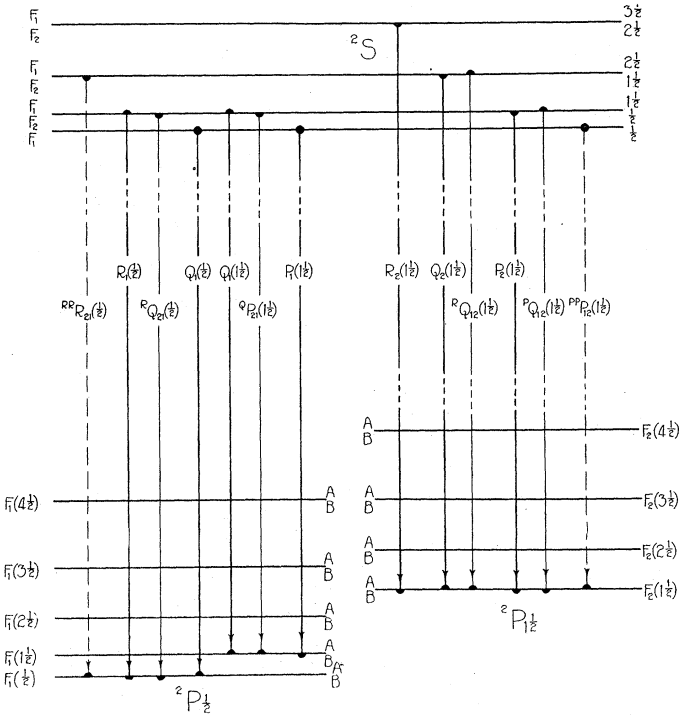

Fig. 5. *Lowest rotational levels, and first lines of each branch, for NO γ band* λ2721 (0, 4 *band*). The levels are drawn to scale with the help of Guillery's Δ_2F data.[41] The relative positions of the ^2S, $^2P_{1\frac{1}{2}}$, and $^2P_{\frac{1}{2}}$ *sets* of levels are, however, not to scale. Doublet separations are all negligible on the scale used, and are shown only by the double designations of the levels. Because of the vanishing ^2S level separations, the satellite branches (light vertical lines) coincide with four of the main branches (heavy vertical lines).

σ-type doubling. According to Guillery's data, the following relations hold.[42,43]

$$R_{21}(j)-R_1(j)\sim Q_1(j+2)-P_1(j+2)<R_1(j+1)-Q_1(j+1) \tag{10}$$

$$R_2(j)-Q_2(j)\gtrsim P_2(j+2)-P_{12}(j+2)<Q_2(j+1)-P_2(j+1) \tag{11}$$

The inequalities indicated in these equations are very slight, especially those in Eq. (11), where it is possible that they represent nothing more than experimental error. Eq. (10) shows (cf. Fig. 5 and Ref. 44) that the relation $F_{1A}''(j)>F_{1B}''(j)$ holds, and from the original data we find $F_{1A}''(j)-F_{1B}''(j)\sim 0.01j''$. Similarly from Eq. (11) and the original data we find $F_{2A}''(j)\geqq F_{2B}''(j)$, the inequality, if any, being very slight.

[42] In Guillery's notation, Eqs. (10) and (11) may be expressed as follows: $c\sim b<a$, where $c=R_i'(m+1)-R_i(m)$, $b=Q_i(m+1)-P_i(m)$, and $a=R_i(m+1)-Q_i(m)$; $i=1$ in her Table 5, 2 in her Table 6.

[43] To avoid confusion, only one symbol has been used even for branches which consist of two superimposed branches: e.g. $R_1(j)$ is intended to imply $R_1(j)$ plus $^RQ_{21}(j)$; all this should be clear from Fig. 5 and Table XI.

NO β *bands.* In the NO β bands ($^2P \rightarrow {}^2P$, with the same final state as the γ bands), the notation which has been used previously[9] is entirely in agreement with the system proposed in VI. The branches observed in these bands are exclusively ordinary *main* branches.

In the NO β bands, the lines of the $^2P_{1/2} \rightarrow {}^2P_{1/2}$ sub-band are doublets of spacing approximately $0.0146j$ (cf. ref. 7, p. 169); assuming $F_{1A}''(j) - F_{1B}''(j) \sim 0.01j''$ from the γ bands, we get $|F_{1A}'(j) - F_{1B}'(j)| \sim 0.025j'$ or $0.005j'$; the two possibilities given, and the order of the A and B levels, cannot be distinguished empirically. In the $^2P_{1\ 1/2} \rightarrow {}^2P_{1\ 1/2}$ band, the lines are single, indicating, since $F_{2A}''(j) \sim F_{2B}''(j)$, that $F_{2A}'(j) \sim F_{2B}'(j)$.

Other Spectra (CN, BO, CO^+)

Intensity relations. The ^2P states of CN, CO^+, and BO form a series with increasing negative values of $\Delta E/B$ (cf. Table II). The values of $\Delta E/B$ here are of the same order of magnitude as those for ZnH and NO, and one therefore expects to find intensity relations in the $^2P \rightarrow {}^2S$ bands of CN, CO^+, and BO similar to those in the ZnH and NO γ bands.

Only the BO α bands have been satisfactorily analyzed in detail.[11] In his analysis of these bands, Jenkins has used a notation conforming with the scheme suggested by the writer in VI. Here, as in the NO γ bands, the ^2S levels $F_1(j+1)$ and $F_2(j)$ are unresolved, hence the four satellite branches coincide with the corresponding main branches. As we should expect from the value of $\Delta E/B$, the unorthodox branches ${}^{RR}R_{21}$ and ${}^{PP}P_{12}$ appear to be distinctly weaker than any of the other branches.

Similar intensity relations exist in the CO^+ comet-tail bands: according to data of Baldet[45] on one of these bands, the intensities of the branches (after altering Baldet's notation to conform with that of the obviously analogous BO α bands) are in the order $[Q_2 + {}^QP_{21}] > [Q_1 + {}^QR_{12}] > [R_2 + {}^RQ_{21}] > [P_1 + {}^PQ_{12}] > R_1 \sim P_2 > {}^{RR}R_{21} > {}^{PP}P_{12}$. The characteristic relation $Q > R > P$ of $P \rightarrow S$ transitions is here also evident.

Intensities of heads. The occurrence of four distinct heads (or six, if the ^2S levels are widely split as in HgH) is typical of both $^2P \rightarrow {}^2S$ and $^2S \rightarrow {}^2P$ bands, in all cases where $|\Delta E|$ or $|\Delta E/B|$ of the ^2P state is large enough to make sensible a division into $^2P_{1/2} \rightarrow {}^2S$ and $^2P_{1\ 1/2} \rightarrow {}^2S$ or $^2S \rightarrow {}^2P_{1/2}$ and $^2S \rightarrow {}^2P_{1\ 1/2}$ sub-bands. It so happens that the first of the four heads, numbering the latter in order in the direction of shading, is always formed by the ${}^{RR}R_{21}$ branch if the bands are shaded toward the red, and by the ${}^{PP}P_{12}$ branch if they are shaded toward the violet; this is true whether the ^2P state

[44] As can best be seen with the help of Fig. 5, noting especially the equality $F_1'(j+1) = F_2'(j)$, the following relations are true: $[c \equiv R_{21}(j) - R_1(j)] = \Delta_1 F_1'(j+1) - \delta_{AB}(j)$; $[b \equiv Q_1(j+2) - P_1(j+2)] = \Delta_1 F_1'(j+1) - \delta_{AB}(j+2)$; $[a \equiv R_1(j+1) - Q_1(j+1)] = \Delta_1 F_1'(j+1) + \delta_{AB}(j+1)$. Here $\delta_{AB}(j)$ mean $F_A''(j) - F_B''(j)$. The experimental relation $c \backsim b$ shows that $\delta_{AB}(j) \backsim \delta_{AB}(j+2)$; we may then take $(c+b)/2$ as practically equal to $\delta_{AB}(j+1)$. The following relation should then hold: $(a-c) \backsim (a-b) \backsim [a-(b+c)/2] = 2\delta_{AB}(j+1)$. Thus from the quantities a, b, c of Guillery's tables,[42] values of $\delta_{AB}(j)$ can be estimated for the F_1'' levels. A similar treatment applies to the quantities in Eq. (11), with the conclusion given in the text.

[45] Cf. F. Baldet, Compt. Rend. **180,** 820 (1925): Thèse Paris 1926.

is initial or final, normal or inverted, as the reader can prove to his own satisfaction by drawing diagrams for all the possible cases. The second and fourth heads are always formed by strong (main plus satellite) branches, the third by a main branch. Thus the relative intensity of the first as compared with the other heads should be an index of $|\Delta E/B|$.

The expected relations are well shown in the series OH, CN, CO^+, BO. Since the P,S bands of these molecules are all shaded toward the red, the first head in each is an ${}^{RR}R_{21}$ head. In OH this is relatively extremely weak and was long unrecognized (cf. above, "seventh non-satellite branch in OH bands"). In CN, it is much stronger than in OH, but is still much weaker than the other three heads.[46] In CO^+ and BO, the first head, while weaker than the other three, is comparable with them in intensity.[11,45]

σ-type doubling in BO. As Jenkins has shown, the relations $F_{1B}'(j) = F_{1A}'(j)$ and $F_{2B}'(j) > F_{2A}'(j)$ hold in BO; in the latter case, the doublet separation is approximately $0.026j$, from the data of ref. 11, Table 1.

WASHINGTON SQUARE COLLEGE,
NEW YORK UNIVERSITY,
June 5, 1928.

[46] Cf. photographs of A. Fowler and H. Shaw, Proc. Roy. Soc. **86***A*, 118 (1912).